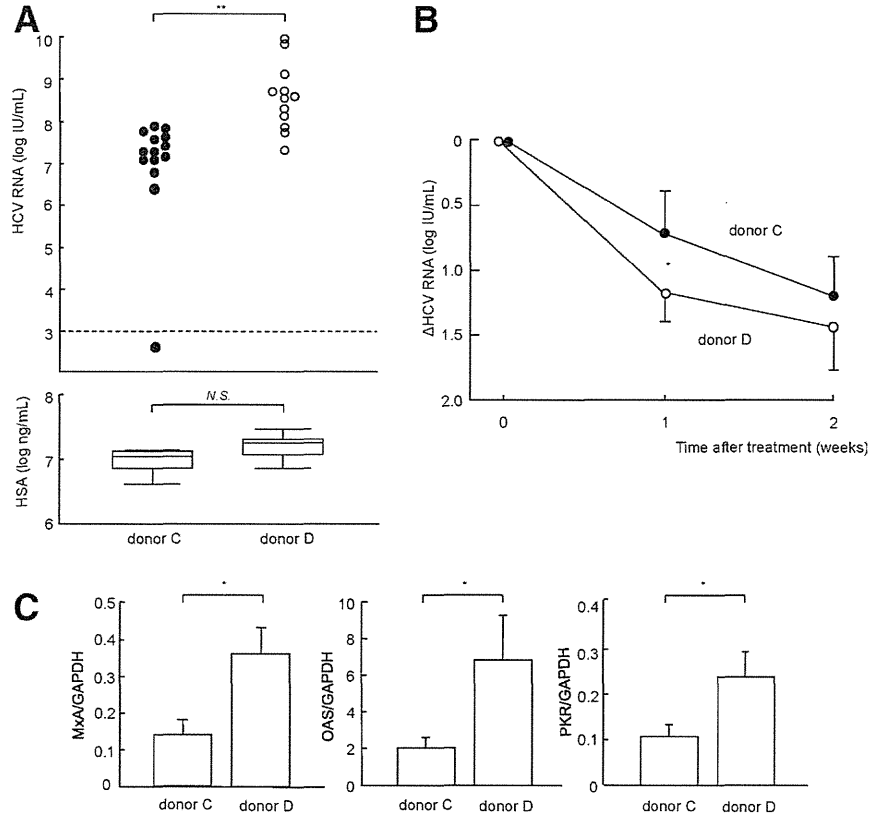

Fig. 4. HCV infectivity, replication ability, and IFN susceptibility in HCV-infected mice. Mice that underwent transplantation with hepatocytes from donor C (rs8099917 TG and rs12979860 TT) (closes circles, n = 14) or D (rs8099917 TT and rs12979860 CC) (open circles, n = 12) were intravenously injected with HCV-infected patient serum samples. (A) Eight weeks after infection, serum HCV RNA titers (upper panel) and HSA concentrations (lower panel) were measured. The horizontal dotted line indicates the HCV RNA titer detection limit (1000 copies/mL). In these box-and-whisker plots, lines within the boxes represent median values; the upper and lower lines of the boxes represent the 75th and 25th percentiles, respectively; the upper and lower bars outside the boxes represent the 90th and 10th percentiles, respectively. HCV-infected mice with hepatocytes from donor C (closed circles, n = 5) or D (open circles, n = 4) were treated daily with 1000 IU/g/day of IFN-alpha for 2 weeks. (B) Changes in mice serum HCV RNA titers measured after 1 and 2 weeks are shown. (C) Intrahepatic ISG expression levels in the IFN-treated mice with donor C (n = 4) or D (n = 3) were measured and expressed relative to GAPDH messenger RNA. Data are reported as mean ± standard deviation. $*P < 0.05$, $**P < 0.01$; NS, not significant.

ISDR, which have been reported to be associated with the outcome of IFN plus ribavirin combination therapy.[8-14] Clones with core aa70 and 91 substitutions showed comparable infection and replication abilities, whereas clones with substitutions in the ISDR showed reduced infectivity and replication rates. It has been reported that patients infected with HCV strains with multiple substitutions in the ISDR have lower viral titers than those with wild-type ISDR, and that these patients respond well to IFN therapy.[8,9] We showed, in this study, that infectivity and replication ability of HCV are apparently impaired in ISDR mutants (Fig. 2A,C). This may explain, at least partially, the better effect of IFN therapy in patients with multiple ISDR mutations. However, why aa substitutions in this particular region are associated with the effect of IFN still remains to be elucidated. In contrast, aa substitutions in the core, which more profoundly affect the outcome of combination therapy,[10-13] did not influence the infectivity and replication ability of the virus (Fig. 2A,B). This suggests that aa substitutions in this region affect response to therapy in a way that is independent of the replication level of the virus. A recent report by Eng et al.[36] showed that a mutation in core aa91 results in the production of minicore protein, which might alter the effect of IFN. The presence of minicore protein and its effect on IFN therapy should be further investigated using the chimeric mouse model.

In contrast to these viral substitutions, host IL28B genotype significantly affected viral replication levels (Figs. 3A and 4A). Curiously, replication levels of the virus are higher in mice with human hepatocytes from donors with rs8099917 TT and rs12979860 CC genotypes, even though these genotypes are associated with successful response to the therapy.[20-22] This result is consistent with clinical observation of higher viral loads in patients with the rs12979860 CC genotype.[20] The favorable IL28B genotype is associated not only with successful response to IFN treatment, but also to spontaneous clearance of the virus.[37,38] However, the incidence of HCV infection was similar in mice with hepatocytes from donors with rs8099917 TT and rs8099917 TG (Figs. 3A and 4A), suggesting that spontaneous clearance was rare. The fact that our animal model was immunodeficient suggests that spontaneous clearance of HCV might require the involvement of the adaptive immune system. The wild-type core protein, aa70, is reported to be found more often in patients with the rs8099917 TT genotype,[23,24] even though patients with this genotype are more likely to be able to eradicate the virus without therapy during

the natural course of infection.[37,38] These data suggest that core aa70 wild-type virus can be eradicated more easily in the natural course of infection, especially in patients with rs8099917 TT or rs12979860 CC genotypes; but once the infection is established, core aa70 wild type replicates more effectively than core aa70 mutant strains.

The effect of IFN on reduction of the virus did not differ between core aa70 wild-type and mutant strains, which showed similar replication levels (Fig. 2D). This is in contrast to clinical observations that the effect of therapy on viral reduction is more prominent in patients with wild-type core protein.[13,25] One of the differences between the mouse model and human patients is term of infection. Long-term HCV infection results in alteration of lipid metabolism and accumulation of lipids in hepatocytes.[39] Patients with fatty change of the liver often fail to respond to therapy.[40] We observed no severe fatty change in mouse livers, suggesting that such long-term change might be absent in this mouse model (data not shown).

On the other hand, the effect of IFN was significantly greater in mice with hepatocytes with the eradication-favorable IL28B genotype (rs8099917 TT and rs12979860 CC) (Figs. 3B and 4B), despite the higher replication rate of the virus. This suggests that the IL28B genotype affects the outcome of therapy based on a different mechanism than viral replication. Because of strong linkage disequilibrium, genotypes of the SNPs around the two IL28B landmark SNPs (rs8099917 and rs12979860) were identical between donors A and C as well as between B and D (data not shown). Further study using human hepatocytes with various IL28B SNP genotypes will identify a primary SNP that directly affects the outcome of therapy. Response to IFN was associated with higher expression levels of ISGs, including MxA, OAS, and PKR (Fig. 4C). This is in agreement with previous studies showing that SVR is associated with stronger induction of ISG expression.[41] However, we observed no statistically significant differences in ISG expression levels from the IL28B SNP genotype before therapy (data not shown). This may result from lower ISG expression levels before therapy and the relatively small number of mice examined. Because there is no adaptive immune system in this mouse model, such differences primarily involve individual hepatocytes, although whether the presence of immune cells enhances this difference should be investigated further.

In summary, we demonstrated that viral infectivity and replication ability are associated with hepatocyte IL28B genotype and are not associated with viral substitutions in the core protein or ISDR. Understanding the mechanism underlying the higher, more prolonged expression of antiviral genes in response-favorable hepatocytes will help us to develop improved therapeutic regimens to eradicate HCV more effectively.

Acknowledgment: We thank Rie Akiyama, Kiyomi Toyota, and Yoko Matsumoto for their expert technical help.

References

1. Kiyosawa K, Sodeyama T, Tanaka E, Gibo Y, Yoshizawa K, Nakano Y, et al. Interrelationship of blood transfusion, non-A, non-B hepatitis, and hepatocellular carcinoma: analysis by detection of antibody to hepatitis C virus. HEPATOLOGY 1990;12:671-675.
2. Niederau C, Lange S, Heintges T, Erhardt A, Buschkamp M, Hürter D, et al. Prognosis of chronic hepatitis C: results of a large, prospective cohort study. HEPATOLOGY 1998;28:1687-1695.
3. Fried MW, Shiffman ML, Reddy KR, Smith C, Marinos G, Gonçales FL Jr, et al. Peginterferon alfa-2a plus ribavirin for patients with chronic hepatitis C virus infection. N Engl J Med 2002;347:975-982.
4. Hoofnagle JH, Ghany MG, Kleiner DE, Doo E, Heller T, Promrat K, et al. Maintenance therapy with ribavirin in patients with chronic hepatitis C who fail to respond to combination therapy with interferon alfa and ribavirin. HEPATOLOGY 2003;38:66-74.
5. Manns MP, McHutchison JG, Gordon SC, Rustgi VK, Shiffman M, Reindollar R, et al. Peginterferon alfa-2b plus ribavirin compared with interferon alfa-2b plus ribavirin for initial treatment of chronic hepatitis C: a randomised trial. Lancet 2001;358:958-965.
6. Fried MW, Shiffman M, Sterling RK, Weinstein J, Crippin J, Garcia G, et al. A multicenter, randomized trial of daily high-dose interferon-alfa 2b for the treatment of chronic hepatitis C: pretreatment stratification by viral burden and genotype. Am J Gastroenterol 2000;95: 3225-3229.
7. McHutchison JG, Gordon SC, Schiff ER, Shiffman ML, Lee WM, Rustgi VK, et al. Interferon alfa-2b alone or in combination with ribavirin as initial treatment for chronic hepatitis C. N Engl J Med 1998; 339:1485-1492.
8. Enomoto N, Sakuma I, Asahina Y, Kurosaki M, Murakami T, Yamamoto C, et al. Mutations in the nonstructural protein 5A gene and response to interferon in patients with chronic hepatitis C virus 1b infection. N Engl J Med 1996;334:77-81.
9. Chayama K, Tsubota A, Kobayashi M, Okamoto K, Hashimoto M, Miyano Y, et al. Pretreatment virus load and multiple amino acid substitutions in the interferon sensitivity-determining region predict the outcome of interferon treatment in patients with chronic genotype 1b hepatitis C virus infection. HEPATOLOGY 1997;25:745-749.
10. Akuta N, Suzuki F, Sezaki H, Suzuki Y, Hosaka T, Someya T, et al. Association of amino acid substitution pattern in core protein of hepatitis C virus genotype 1b high viral load and non-virological response to interferon-ribavirin combination therapy. Intervirology 2005;48: 372-380.
11. Akuta N, Suzuki F, Kawamura Y, Yatsuji H, Sezaki H, Suzuki Y, et al. Predictive factors of early and sustained responses to peginterferon plus ribavirin combination therapy in Japanese patients infected with hepatitis C virus genotype 1b: amino acid substitutions in the core region and low-density lipoprotein cholesterol levels. J Hepatol 2007;46: 403-410.
12. Akuta N, Suzuki F, Hirakawa M, Kawamura Y, Yatsuji H, Sezaki H, et al. A matched case-controlled study of 48 and 72 weeks of peginterferon plus ribavirin combination therapy in patients infected with HCV genotype 1b in Japan: amino acid substitutions in HCV core region as predictor of sustained virological response. J Med Virol 2009; 81:452-458.

13. Mori N, Imamura M, Kawakami Y, Saneto H, Kawaoka S, Takaki S, et al. Randomized trial of high-dose interferon-alpha-2b combined with ribavirin in patients with chronic hepatitis C: correlation between amino acid substitutions in the core/NS5A region and virological response to interferon therapy. J Med Virol 2009;81:640-649.
14. Okanoue T, Itoh Y, Hashimoto H, Yasui K, Minami M, Takehara T, et al. Predictive values of amino acid sequences of the core and NS5A regions in antiviral therapy for hepatitis C: a Japanese multi-center study. J Gastroenterol 2009;44:952-963.
15. Welzel TM, Morgan TR, Bonkovsky HL, Naishadham D, Pfeiffer RM, Wright EC, et al. Variants in interferon-alpha pathway genes and response to pegylated interferon-alpha2a plus ribavirin for treatment of chronic hepatitis C virus infection in the hepatitis C antiviral long-term treatment against cirrhosis trial. HEPATOLOGY 2009;49:1847-1858.
16. Hijikata M, Ohta Y, Mishiro S. Identification of a single nucleotide polymorphism in the MxA gene promoter (G/T at nt -88) correlated with the response of hepatitis C patients to interferon. Intervirology 2000;43:124-127.
17. Knapp S, Yee LJ, Frodsham AJ, Hennig BJ, Hellier S, Zhang L, et al. Polymorphisms in interferon-induced genes and the outcome of hepatitis C virus infection: roles of MxA, OAS-1, and PKR. Genes Immun 2003;4:411-419.
18. Matsuyama N, Mishiro S, Sugimoto M, Furuichi Y, Hashimoto M, Hijikata M, et al. The dinucleotide microsatellite polymorphism of the IFNAR1 gene promoter correlates with responsiveness of hepatitis C patients to interferon. Hepatol Res 2003;25:221-225.
19. Naito M, Matsui A, Inao M, Nagoshi S, Nagano M, Ito N, et al. SNPs in the promoter region of the osteopontin gene as a marker predicting the efficacy of interferon-based therapies in patients with chronic hepatitis C. J Gastroenterol 2005;40:381-388.
20. Ge D, Fellay J, Thompson AJ, Simon JS, Shianna KV, Urban TJ, et al. Genetic variation in IL28B predicts hepatitis C treatment-induced viral clearance. Nature 2009;461:399-401.
21. Suppiah V, Moldovan M, Ahlenstiel G, Berg T, Weltman M, Abate ML, et al. IL28B is associated with response to chronic hepatitis C interferon-alpha and ribavirin therapy. Nat Genet 2009;41:1100-1104.
22. Tanaka Y, Nishida N, Sugiyama M, Kurosaki M, Matsuura K, Sakamoto N, et al. Genome-wide association of IL28B with response to pegylated interferon-alpha and ribavirin therapy for chronic hepatitis C. Nat Genet 2009;41:1105-1109.
23. Abe H, Ochi H, Maekawa T, Hayes CN, Tsuge M, Miki D, et al. Common variation of IL28 affects gamma-GTP levels and inflammation of the liver in chronically infected hepatitis C virus patients. J Hepatol 2010;53:439-443.
24. Akuta N, Suzuki F, Hirakawa M, Kawamura Y, Yatsuji H, Sezaki H, et al. Amino acid substitution in hepatitis C virus core region and genetic variation near the interleukin 28B gene predict viral response to telaprevir with peginterferon and ribavirin. HEPATOLOGY 2010;52:421-429.
25. Hayes CN, Kobayashi M, Akuta N, Suzuki F, Kumada H, Abe H, et al. HCV substitutions and IL28B polymorphisms on outcome of peg-interferon plus ribavirin combination therapy. Gut 2011;60:261-267.
26. Mercer DF, Schiller DE, Elliott JF, Douglas DN, Hao C, Rinfret A, et al. Hepatitis C virus replication in mice with chimeric human livers. Nat Med 2001;7:927-933.
27. Kneteman NM, Weiner AJ, O'Connell J, Collett M, Gao T, Aukerman L, et al. Anti-HCV therapies in chimeric scid-Alb/uPA mice parallel outcomes in human clinical application. HEPATOLOGY 2006;43:1346-1353.
28. Kamiya N, Iwao E, Hiraga N, Tsuge M, Imamura M, Takahashi S, et al. Practical evaluation of a mouse with chimeric human liver model for hepatitis C virus infection using an NS3-4A protease inhibitor. J Gen Virol 2010;91:1668-1677.
29. Tateno C, Yoshizane Y, Saito N, Kataoka M, Utoh R, Yamasaki C, et al. Near completely humanized liver in mice shows human-type metabolic responses to drugs. Am J Pathol 2004;165:901-912.
30. Vanwolleghem T, Libbrecht L, Hansen BE, Desombere I, Roskams T, Meuleman P, et al. Factors determining successful engraftment of hepatocytes and susceptibility to hepatitis B and C virus infection in uPA-SCID mice. J Hepatol 2010;53:468-476.
31. Hiraga N, Imamura M, Tsuge M, Noguchi C, Takahashi S, Iwao E, et al. Infection of human hepatocyte chimeric mouse with genetically engineered hepatitis C virus and its susceptibility to interferon. FEBS Letts 2007;581:1983-1987.
32. Kimura T, Imamura M, Hiraga N, Hatakeyama T, Miki D, Noguchi C, et al. Establishment of an infectious genotype 1b hepatitis C virus clone in human hepatocyte chimeric mice. J Gen Virol 2008;89:2108-2113.
33. Ohnishi Y, Tanaka T, Ozaki K, Yamada R, Suzuki H, Nakamura Y. A high-throughput SNP typing system for genome-wide association studies. J Hum Genet 2001;46:471-477.
34. Suzuki A, Yamada R, Chang X, Tokuhiro S, Sawada T, Suzuki M, et al. Functional haplotypes of PADI4, encoding citrullinating enzyme peptidylarginine deiminase 4, are associated with rheumatoid arthritis. Nat Genet 2003;34:395-402.
35. Kato T, Matsumura T, Heller T, Saito S, Sapp RK, Murthy K, et al. Production of infectious hepatitis C virus of various genotypes in cell cultures. J Virol 2007;81:4405-4411.
36. Eng FJ, Walewski JL, Klepper AL, Fishman SL, Desai SM, McMullan LK, et al. Internal initiation stimulates production of p8 minicore, a member of a newly discovered family of hepatitis C virus core protein isoforms. J Virol 2009;83:3104-3114.
37. Thomas DL, Thio CL, Martin MP, Qi Y, Ge D, O'Huigin C, et al. Genetic variation in IL28B and spontaneous clearance of hepatitis C virus. Nature 2009;461:798-801.
38. Montes-Cano MA, García-Lozano JR, Abad-Molina C, Romero-Gómez M, Barroso N, Aguilar-Reina J, et al. Interleukin-28B genetic variants and hepatitis virus infection by different viral genotypes. HEPATOLOGY 2010;52:33-37.
39. Lonardo A, Adinolfi LE, Loria P, Carulli N, Ruggiero G, Day CP. Steatosis and hepatitis C virus: mechanisms and significance for hepatic and extrahepatic disease. Gastroenterology 2004;126:586-597.
40. Poynard T, Ratziu V, McHutchison J, Manns M, Goodman Z, Zeuzem S, et al. Effect of treatment with peginterferon or interferon alfa-2b and ribavirin on steatosis in patients infected with hepatitis C. HEPATOLOGY 2003;38:75-85.
41. Sarasin-Filipowicz M, Oakeley EJ, Duong FH, Christen V, Terracciano L, Filipowicz W, et al. Interferon signaling and treatment outcome in chronic hepatitis C. Proc Natl Acad Sci U S A 2008;105:7034-7039.

THE JOURNAL OF BIOLOGICAL CHEMISTRY VOL. 287, NO. 46, pp. 38716–38728, November 9, 2012

Matrix Metalloproteinase-13 (MMP-13) Directly and Indirectly Promotes Tumor Angiogenesis*

Received for publication, April 17, 2012, and in revised form, September 10, 2012 Published, JBC Papers in Press, September 19, 2012, DOI 10.1074/jbc.M112.373159

Yasusei Kudo[‡§1], Shinji Iizuka[‡], Maki Yoshida[‡], Takaaki Tsunematsu[‡], Tomoyuki Kondo[§], Ajiravudh Subarnbhesaj[‡], Elsayed M. Deraz[‡], Samadarani B. S. M. Siriwardena[‡], Hidetoshi Tahara[¶], Naozumi Ishimaru[§], Ikuko Ogawa[‖], and Takashi Takata[‡2]

From the [‡]Department of Oral and Maxillofacial Pathobiology and [¶]Department of Cellular and Molecular Biology, Graduate School of Biomedical Sciences, Hiroshima University, and the [‖]Center of Oral Clinical Examination, Hiroshima University Hospital, Hiroshima 734-8553, Japan and the [§]Department of Oral Molecular Pathology, Institute of Health Biosciences, The University of Tokushima Graduate School, Tokushima 770-8504, Japan

Background: Angiogenesis is an important step in the metastatic cascade of tumors.
Results: MMP-13 itself as well as VEGF-A secretion from fibroblasts promotes angiogenesis. Indeed, MMP-13 is well correlated with blood vessel density in human cancer tissues.
Conclusion: MMP-13 can be a marker for prediction of malignant behaviors and a therapeutic target in cancer.
Significance: This work provides new insights regarding the role of MMP-13 in tumor angiogenesis.

Matrix metalloproteinases (MMPs) are extracellular zinc-dependent endopeptidases involved in the degradation and remodeling of extracellular matrix in physiological and pathological processes. MMPs also have a role in cell proliferation, migration, differentiation, angiogenesis, and apoptosis. We previously identified cancer invasion-related factors by comparing the gene expression profiles between parent and the highly invasive clone of cancer cells. Matrix metalloproteinase-13 (MMP-13) was identified as a common up-regulated gene by cancer invasion-related factors. Although MMP-13 slightly promoted tumor invasion, we found that MMP-13 was involved in tumor angiogenesis. Conditioned medium from MMP-13-overexpressing cells promoted capillary formation of immortalized human umbilical vein endothelial cells. Furthermore, treatment with recombinant MMP-13 protein enhanced capillary tube formation both *in vitro* and *in vivo*. MMP-13-promoted capillary tube formation was mediated by activation of focal adhesion kinase and ERK. Interestingly, MMP-13 promoted the secretion of VEGF-A from fibroblasts and endothelial cells. By immunohistochemical analysis, we found a possible correlation between MMP-13 expression and the number of blood vessels in human cancer cases. In summary, these findings suggest that MMP-13 may directly and indirectly promote tumor angiogenesis.

The process of metastasis consists of sequential and selective steps, including proliferation, induction of angiogenesis, detachment, motility, invasion into circulation, aggregation and survival in the circulation, cell arrest in distant capillary beds and extravasation into organ parenchyma (1, 2). Induction of angiogenesis is considered one of the important steps in the metastatic cascade of tumors. It is widely accepted that tumor growth and metastasis are angiogenesis-dependent, and hence, blocking angiogenesis could be a strategy to arrest tumor growth (3). The "angiogenic switch" is "off" when the effect of proangiogenic molecules is balanced by that of anti-angiogenic molecules, and is "on" when the net balance is tipped in favor of angiogenesis (4, 5). Pro- and anti-angiogenic molecules can be emanated from cancer cells, endothelial cells, stromal cells, blood, and the extracellular matrix (ECM)[3] (6). Their relative contribution is likely to change with tumor type and site. It is also likely to change with tumor growth, regression and relapse. However, the interplay between environmental and genetic mechanisms influencing tumor angiogenesis and growth is a complex and largely unresolved matter.

The ECM undergoes significant remodeling during tumor progression and this is mediated largely by the extracellular proteinases, particularly the matrix metalloproteinases (MMPs), and the major source of these is from the stromal cells (7). MMPs represent a family of zinc-dependent proteinases, which are able to degrade ECM components such as collagens and proteoglycans and have a role in normal development and tissue damage in various pathophysiological conditions involving arthritis, wound healing, and tumor development (8). MMPs can be classified into subgroups, including collagenases, stromelysins, gelatinases, and membrane-type MMPs (9). MMPs have been implicated in the promotion of tumor inva-

* This work was supported by grants-in-aid from the Ministry of Education, Science, and Culture of Japan (to Y. K. and T. Ta.), a research fellowship for Young Scientists and the Excellent Young Researchers Overseas Visit Program from the Japan Society for the Promotion of Science (to S. I. and T. Ts.), and a Kurozumi Memorial Foundation grant (to Y. K.).

[1] To whom correspondence may be addressed: Dept. of Oral Molecular Pathology, Institute of Health Biosciences, The University of Tokushima Graduate School, Tokushima, 3-18-15 Kuramoto, Tokushima 770-8504, Japan. Fax: 81-88-633-7328; E-mail: yasusei@tokushima-u.ac.jp.

[2] To whom correspondence may be addressed: Dept. of Oral and Maxillofacial Pathobiology, Division of Frontier Medical Science, Graduate School of Biomedical Sciences, Hiroshima University, 1-2-3 Kasumi, Minami-ku, Hiroshima 734-8553, Japan. Fax: 81-82-257-5619; E-mail: ttakata@hiroshima-u.ac.jp.

[3] The abbreviations used are: ECM, extracellular matrix; MMP, matrix metalloproteinase; VEGF, vascular endothelial growth factor; FAK, focal adhesion kinase; HUVEC, human umbilical vein endothelial cell; HNSCC, head and neck squamous cell carcinoma; TGF-β, transforming growth factor-β: α-SMA, α-smooth muscle actin.

sion and metastasis for decades (10). It is now evident that MMP function is more complex than initially thought, given that these enzymes do more than degrade physical barriers. MMPs also affect multiple signaling pathways that modulate the biology of the cell in normal physiological processes and in disease. It is now evident that some MMPs such as MMP-1, -2, -3, -7, -9, -14, and -16 can contribute to distinct vascular events in tumors (11). Among them, MMP-9, conveyed by inflammatory cells, has a distinct role in tumor angiogenesis, mainly regulating the bioavailability of VEGF. MMP-9 enables an angiogenic switch by making sequestered VEGF bioavailable for its receptor VEGFR-2 in pancreatic islet tumors (12). In addition, the direct cleavage of matrix-bound VEGF by MMP-3, -7, -9, or -16 results in modified VEGF molecules with altered bioavailability, which changes the vascular patterning of tumors *in vivo* (13). However, the degradation of ECM components and other extracellular molecules may generate fragments with new bioactivities that inhibit angiogenesis (14). Thus, MMPs have dual functions as inhibiting and promoting angiogenesis, and the effects of MMPs on angiogenesis might be diverse.

It has recently been shown that a repair of bone fracture in MMP-13-deficient mice is delayed, which suggests a critical role of MMP-13 in the process of angiogenesis during the healing of fracture (15). Additionally, chicken MMP-13 was shown to directly contribute to neovascularization, which clearly extends the physiologic role of MMP-13 associated with cartilage and bone resorption to collagen remodeling in the angiogenic process (16). MMP-13 is known as collagenase-3 and is active against a wide variety of ECM components (17). Moreover, high expression of MMP-13 has been related to tumor behavior and prognosis (18). Recently, it has been shown that MMP-13 produced from stromal fibroblasts promotes angiogenesis through increased protein level of VEGF and VEGFR-2 in cancer invasive area (19). Here, we found that MMP-13 produced by cancer cells directly and indirectly promoted tumor angiogenesis.

EXPERIMENTAL PROCEDURES

Reagents—Active form of recombinant human MMP-13, which truncated from the C terminus was obtained from Chondrex, Inc. (Redmond, WA). This recombinant protein was made using the pET vector system in *Escherichia coli*. Recombinant TGF-β and ERK inhibitor, U0126 was obtained from R&D Systems (Minneapolis, MN). Focal adhesion kinase (FAK) inhibitor, FAK inhibitor 14, was obtained from Santa Cruz Biotechnology (Santa Cruz, CA). MMP-13 inhibitor, CL82198, was obtained from Merck Millipore (Darmstadt, Germany).

Cell Lines and Culture Conditions—Head and neck squamous cell carcinoma (HNSCC) cell lines (HCS2, HSC3, HSC4, Ca-9-22, Ho-1-N-1, and Ho-1-U-1) were provided by the Japanese Collection of Research Bioresources Cell Bank. These cells were maintained in RPMI 1640 (Nacalai tesque, Inc., Kyoto, Japan) supplemented with 10% heat-inactivated FBS (Invitrogen) and 100 units/ml penicillin-streptomycin (Invitrogen) under the condition of 5% CO_2 in air at 37 °C. Immortalized human umbilical vein endothelial cells (HUVECs; HuhT1 cells) were used in this study. HuhT1 cells were previously established by transfection with human telomerase reverse transcriptase (20). HuhT1 cells was maintained in HuMedia-EG2 (Kurabo, Okayama, Japan) under the condition of 5% CO_2 in air at 37 °C. Normal fibroblasts were obtained from gingival tissues using standard explant techniques (21). The tissues were obtained undergoing routine dental surgery in the Department of Oral Surgery (Hiroshima University Hospital). Normal fibroblasts were maintained in DMEM supplemented with 10% FBS. Only cells between passages three and five were used in this study.

RT-PCR—Using RNeasy mini kit (Qiagen, Hilden, Germany), total RNA from cultures of confluent cells was isolated. These isolates were quantified and their purity was evaluated by spectrophotometer. The cDNA was synthesized from 1 μg of total RNA according to ReverTra Dash (Toyobo Biochemicals, Tokyo, Japan). We used the following primers: human MMP-13, 5′-ttgagctggactcattgtcg-3′ (forward) and 5′-ggagcctctcagtcatggag-3′ (reverse); human glyceraldehyde-3-phosphate dehydrogenase (GAPDH), 5′-tccaccaccctgttgctgta-3′ (forward) and 5′-accacagtccatgccatcac-3′ (reverse). Aliquots of total cDNA were amplified with 1.25 units of rTaq-DNA polymerase (Qiagen), and this amplification was done in a thermal cycler (MyCyler, Bio-Rad, Richmond, CA) for 30 cycles after initial 30 s of denaturation at 94 °C, annealing for 30 s at 60 °C, and extension for 1 min at 72 °C in all primers used. The amplification reaction products were resolved on 1.2% agarose/TAE gels (Nacalai tesque), electrophoresed at 100 mV, and then finally visualized by using ethidium bromide.

Generation of MMP-13-overexpressing Cells—pcDNA3.1-FLAG-MMP-13 expression vector was kindly provided by Dr. Michael Byrne (Harvard Medical School). We transfected MMP-13 into HSC3 cells. Then, G418 (300 μg/ml; Invivogen, San Diego, CA) was added to the culture medium after 48 h of transfection. After 2 weeks of G418 selection, we obtained the stable pool clones. Cell transfections were performed using FuGENE 6HD (Roche Applied Science) according to the manufacturer's instruction. Conditioned media were collected after incubation with RPMI without FBS for 2 days.

Silencing by siRNA—Logarithmically growing HSC4 and Ho-1-N-1 cells were seeded at a density of 10^5 cells/dish (6 cm) and transfected with 20 nM siRNA by using Oligofectamine® RNAi MAX (Invitrogen), according to the manufacturer's instructions. Forty-eight hours after transfection, the cells were prepared and analyzed by Western blot analysis. At the same time, we changed to new medium, incubated for 48 h, and collected the conditioned medium. The following siRNA oligonucleotides were obtained from B-Bridge International, Inc. (Mountain View, CA): MMP-13, gaugaaaccuggacaaguaTT. A scrambled sequence without significant homology to rat, mouse, or human gene sequences was used as a control.

Western Blot Analysis—Western blotting was carried out as described previously (22). The protein concentrations were measured by Bradford protein assay (Bio-Rad). Twenty μg of protein was subjected to 10% polyacrylamide gel electrophoresis, followed by electroblotting onto a nitrocellulose filter. For detection of the immunocomplex, the ECL Western blotting detection system (Amersham Biosciences) was used. Anti-MMP-13 monoclonal antibody (Fuji Company Industries, Tokyo, Japan), anti-FLAG monoclonal antibody (Sigma), and

anti-β-actin monoclonal antibody (Sigma), α-smooth muscle actin (α-SMA), anti-phospho-FAK (Tyr-576/Tyr-577) monoclonal antibody (Cell Signaling Technology, Beverly, MA), anti-phospho-Src (Tyr-416) polyclonal antibody (Cell Signaling Technology), anti-phospho-ERK (Thr-202/Tyr-204) monoclonal antibody (Santa Cruz Biotechnology, Santa Cruz, CA), anti-FAK polyclonal antibody (Cell Signaling Technology), anti-Src polyclonal antibody (Cell Signaling Technology), and anti-ERK monoclonal antibody (Cell Signaling Technology) were used. For detection of phosphorylated proteins, membranes were blocked with 3% milk/TBS-T and incubated with phospho-specific antibodies overnight at 4 °C. After washing in TBS-T, membranes were incubated with specific secondary antibodies, and the proteins were visualized as described previously.

MMP-13 Activity—The MMP-13 activity was determined by a MMP-13 inhibitor assay kit (Chondrex, Inc., Redmond, WA, distributed by IWAI Chemicals Company, Japan, catalog no. 3003). A designate reaction was performed in the 96-well

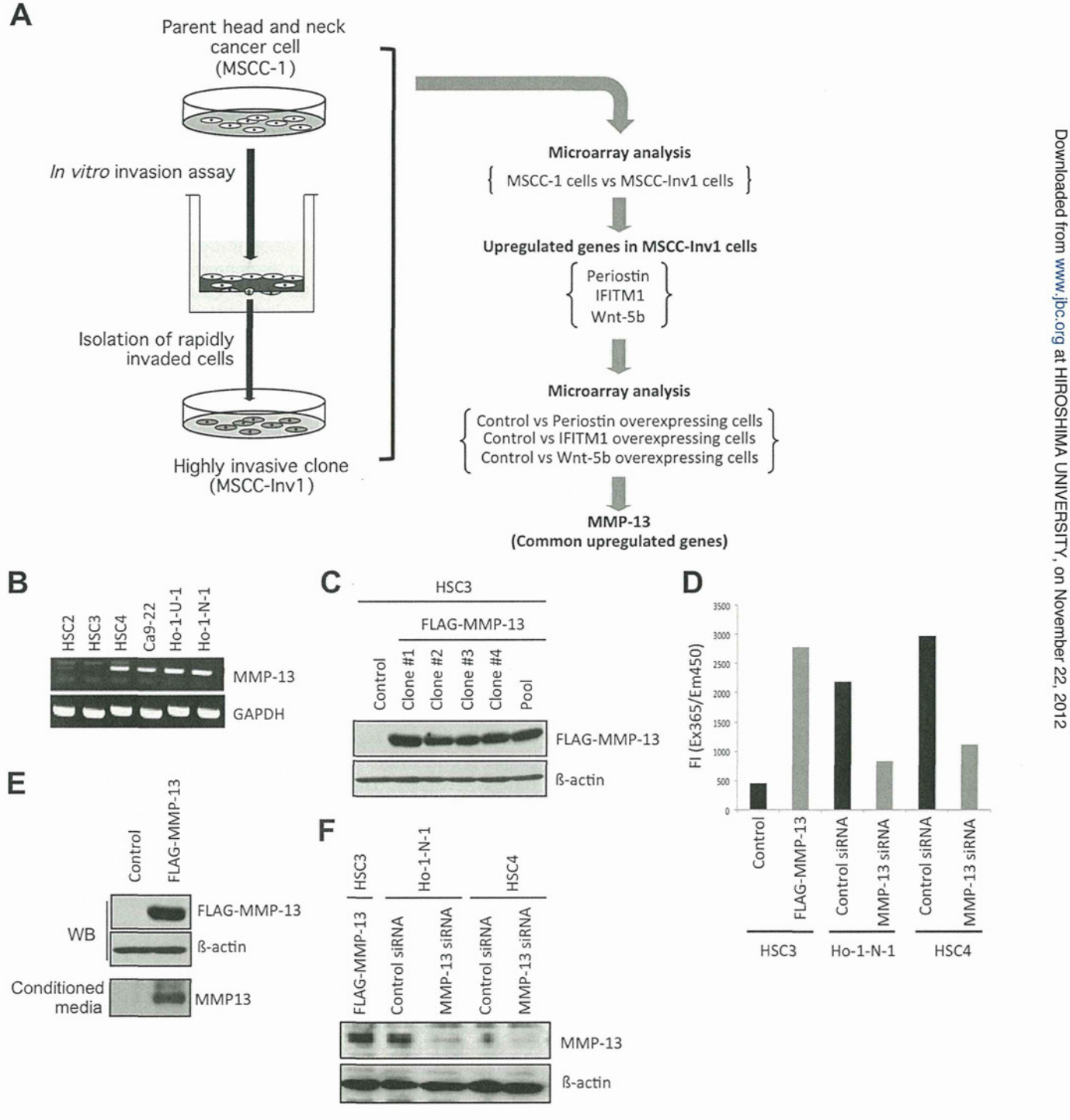

microtiter plate according to the manufacturer's instructions. The assay procedure was separated into two stages. First, diluted recombinant human MMP-13 (10 μg/ml) with dilution buffer B or conditioned medium (from control cells, MMP-13-overexpressing cells or MMP-13 siRNA-treated cells) was activated by adding 5 μl of aminophenylmercuric acetate at 35 °C for 60 min. Second, appropriate amounts of test samples with or without several inhibitors (U0126, FAK inhibitor 14 and CL82198) that diluted by solution B and reaction buffer to the wells were added to adjust the final volume to 160 μl. The reaction was initiated by adding 100 μl of substrate solution to each well. The collagenase reaction was stopped by adding 10 μl of the stop solution to each well after incubating at room temperature for ~30 min. The reaction fluorescence intensity was determined at $\lambda_{emission}$ = 450 nm and $\lambda_{excitation}$ = 345 nm with Varioskan Flash (Thermo Scientific). The MMP-13 activity was determined by comparing with a standard response curve using buffer instead of inhibitor in similar conditions. All assays were carried out in three replications.

Migration Assay—Migration activity was measured by the use of a 24-well cell culture insert with 8-μm pores (Falcon Becton Dickinson). The lower compartment contained 0.5 ml of conditioned medium or serum-free medium with or without 100 ng/ml of recombinant MMP-13. After trypsinization, 5×10^4 cells were resuspended in 100 μl of serum-free medium and placed in the upper compartment of the cell culture insert for 4 h. To examine the activity of migration, the cells that had penetrated onto the lower side of the filter were fixed with formalin and stained with hematoxylin. These were assayed three times.

In Vitro Angiogenesis by HUVECs—An angiogenesis assay kit obtained from Kurabo (Osaka, Japan) was used according to the manufacturer's instructions with minor modifications (23). HUVECs were treated with conditioned medium from MMP-13-overexpressing cells or control cells (1:1 mixture with the medium). HUVECs were also treated with different concentrations of recombinant MMP-13 protein (0, 50, 100 and 200 ng/ml). VEGF-A (2 μg/ml) was used as a positive control, and suramin (1 mM) was used as a negative control. We examined three wells/data point in a single experiment. The media were changed every 3 days. After 12 days, the cells were fixed at room temperature with cold 70% ethanol for 30 min. The cells were incubated with the anti-human CD31 antibody for 1 h at 37 °C and further with an alkaline phosphatase-conjugated goat anti-mouse IgG antibody. Visualization was achieved with 5-bromo-4-chloro-3-indolyl phosphate-nitrobluetetrazolium. Capillary tube score was estimated with the Chalkley count method under a bright-field microscope (24).

Rat Aortic Ring Angiogenesis Assay—The effect of samples on angiogenesis was studied by culturing aortic explants in three-dimensional matrix gels according to the protocol described by Bauer *et al.* (25). Thoracic aorta was excised from 7-week-old male Sprague-Dawley rat, and the fibroadipose tissue was removed. The aorta was sectioned into 1-mm-long cross-sections, rinsed with EBM-2 medium (Lonza, Walkersville, MD), placed on the Matrigel-coated wells, covered with additional 50 μl of Matrigel, and allowed to form a gel for more than 30 min at 37 °C, 5% CO_2. Afterward, control was treated with EBM-2 medium only, and the test sample was treated with EBM-2 medium containing recombinant MMP-13 protein. Each medium was added every other day. All assays were performed by using five aortic rings per sample. Aortic rings were photographed on day 15. The area of angiogenic sprouting was calculated using Image-Pro Plus software program (Media Cybernetics). Microvessel densities were reported in square pixels.

VEGF-A Quantification—A fixed number of fibroblasts cultured in medium without FBS were treated with MMP-13 (0, 10 and 50 ng/ml) and/or TGF-β (1 ng/ml) for 24 h. The concentration of VEGF-A in the culture medium was quantified with commercial ELISA kit according to the manufacturers' instructions (Pierce Biotechnology, Rockford, IL).

Tissue Samples—Sixty-seven tissue samples of human HNSCC were retrieved from the Surgical Pathology Registry of University of Peradeniya and Oral and Maxillofacial unit, Kandy Hospital, after being approved by the Ethical Committee of each institution. Informed consent obtained from all patients was verbal for this study, and then signature was obtained from all patients. Sixty-seven Sri Lankan HNSCC cases (42 male, nine female and 16 unknown; average age was 50.2 ± 13.2) were surgically resected from 1998 to 2004 before radiochemotherapy. Clinical information including metastasis was gathered from surgical records of the patients. Tissues were fixed in 10% buffered formalin and embedded in paraffin.

Immunohistochemistry—Tumor tissues were fixed in 10% formalin, embedded in paraffin, and cut into 4-μm thick sections. For immunohistochemical staining, tissue sections were deparaffinized in xylene and rehydrated in descending grades of ethanol. Endogenous peroxidase activity was blocked with

FIGURE 1. **Identification of MMP-13.** *A*, schema shows the strategy to identify MMP-13. Periostin, IFITM1, and Wnt-5b are identified as the invasion-related molecules by comparing the gene expression profile between the parent (MSCC-1 cells) and a highly invasive clone (MSCC-Inv1 cells). To identify common up-regulated genes, we compared the gene expression profiles of control *versus* periostin-overexpressing cells, control *versus* IFITM1-overexpressing cells, and control *versus* Wnt-5b-overexpressing cells. MMP-13 is commonly up-regulated among periostin-, IFITM1-, and Wnt-5b-overexpressing cells. *B*, expression of MMP-13 in HNSCC cell lines. Expression of MMP-13 mRNA in six HNSCC cell lines: HSC2, HSC3, HSC4, Ca-9-22, Ho-1-N-1, and Ho-1-U-1 was examined by RT-PCR. GAPDH was used as a loading control. *C*, generation of MMP-13-overexpressing cells. pcDNA3.1-FLAG-MMP13 was transfected into HSC3 cells. After selection, we obtained four stable clones and one stable pool clone of MMP-13-overexpressing cells. Ectopic expression of MMP-13 was examined by immunoblotting with an anti-FLAG antibody. In further experiments, clone 1 was used. *D*, MMP-13 ability was determined by a MMP-13 inhibitor assay kit as described under "Experimental Procedures." Conditioned medium was collected from control HSC3, MMP-13-overexpressing HSC3, control Ho-1-N-1, MMP-13 siRNA-treated Ho-1-N-1, control HSC4, and MMP-13 siRNA-treated HSC4 cells. The reaction was initiated by adding 100 μl of substrate solution, and the reaction fluorescence intensity was determined at $\lambda_{emission}$ = 450 nm and $\lambda_{excitation}$ = 345 nm. The graph shows fluorescence intensity. All assays were carried out in three replications. *E*, ectopic expression of FLAG-MMP-13 was examined by immunoblotting with an anti-FLAG antibody. β-Actin expression was used as a loading control. Expression of MMP-13 in condensed conditioned medium was detected by immunoblotting with an anti-MMP-13 antibody. *F*, MMP-13 knockdown in HSC4 and Ho-1-N-1 cells. MMP-13 siRNA was transfected into HSC4 and Ho-1-N-1 cells. A scrambled sequence that does not show significant homology to rat, mouse, or human gene sequences was used as a control. After 48 h, cells were collected, and MMP-13 expression was examined by Western blot (*WB*) analysis. β-Actin expression was used as a loading control.

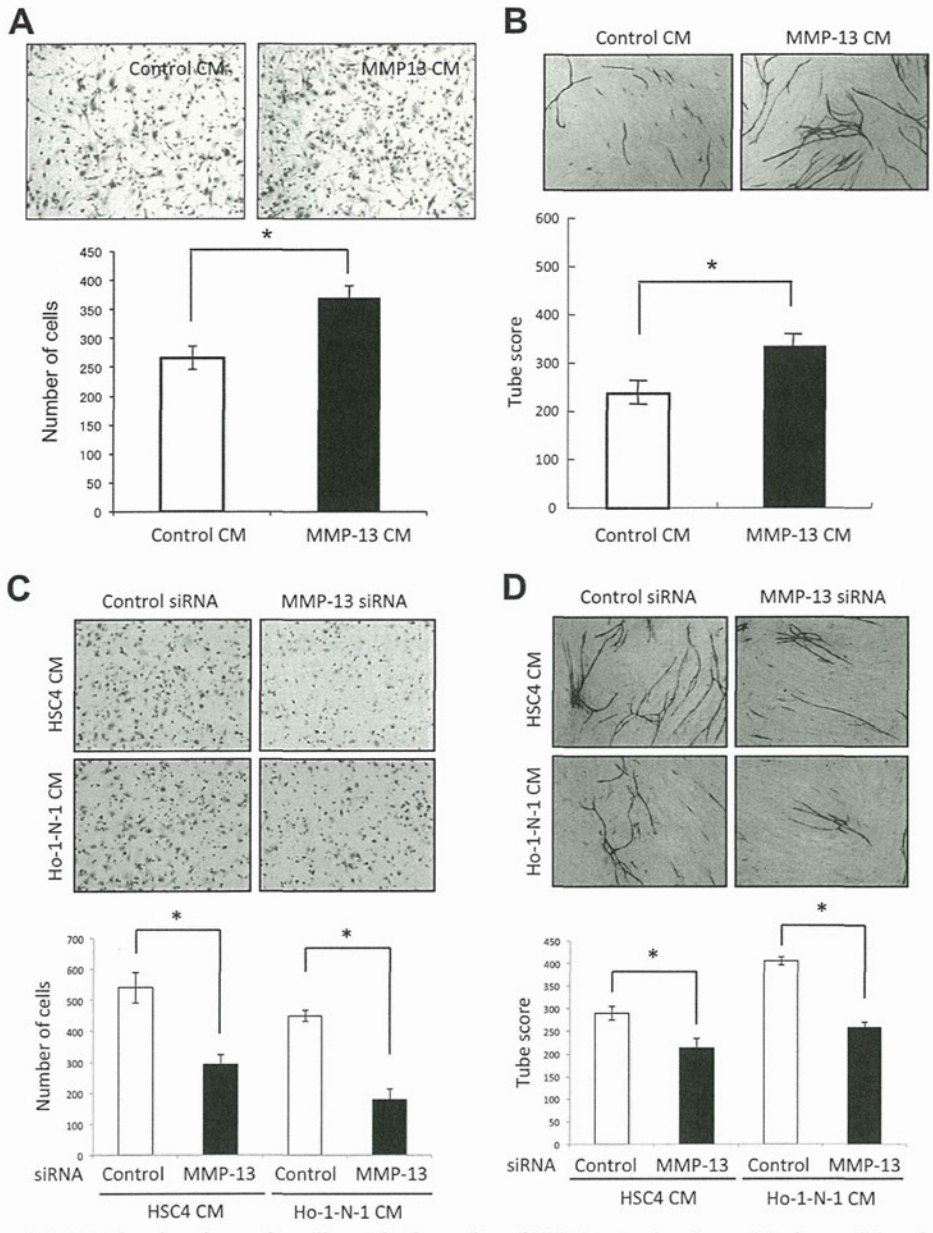

FIGURE 2. **Involvement of MMP-13 in migration and capillary tube formation of HUVECs.** *A*, migration activity by conditioned medium from MMP-13-overexpressing cells. Migration activity was measured by the use of a 24-well cell culture insert with 8-μm pores. The lower compartment contained 0.5 ml of conditioned medium from empty vector-transfected HSC3 cells (control *CM*) or MMP-13-overexpressing HSC3 cells (MMP-13 CM). After trypsinization, 5×10^4 of immortalized HUVECs (HuhT1) were resuspended in 100 μl of serum-free medium and placed in the upper compartment of the cell culture insert for 4 h. To examine the activity of migration, the cells that had penetrated onto the lower side of the filter were fixed with formalin and stained with hematoxylin. The *upper panel* shows the representative area of penetrated cells. The *lower graph* shows the average number of penetrated cells. The *bars* show the average values and S.D. of three independent experiments. *, significantly different from control at $p < 0.05$. *B*, *upper panel* shows the representative area of capillary tube formation by conditioned medium from empty vector-transfected HSC3 cells (control CM) or MMP-13-overexpressing HSC3 cells (MMP-13 CM) (×40). An angiogenesis assay kit was used according to the manufacturer's instructions with minor modifications. HUVECs were treated with mixture of conditioned medium and HuMedia-EG2 in a percentage of 1:1. The mixed media were changed every 3 days. After 12 days, the cells were fixed and stained with anti-human CD31 antibody as described under "Materials and Methods." The *lower graph* shows the average capillary tube score after conditioned medium treatment. Capillary tube score was estimated with the Chalkley count method under a bright-field microscope. The values represent means of capillary tube score + S.D. based on three wells/data point in a single experiment. *, significantly different from control at $p < 0.05$. *C*, migration activity of HuhT1 cells by conditioned medium from control or MMP-13 siRNA-treated cells. MMP-13 siRNA were transfected into HSC4 and Ho-1-N-1 cells. Migration activity was measured as described in *A*. The *upper panel* shows the representative area of penetrated cells. The *lower graph* shows the average number of penetrated cells. The *bars* show the average values and S.D. of three independent experiments. *, significantly different from control at $p < 0.05$. *D*, upper panel shows the representative area of capillary tube formation by conditioned medium from control or MMP-13-depleted cells (×40). Capillary tube formation was examined as described in *B*. The *lower graph* shows the average capillary tube score after conditioned medium treatment. Capillary tube score was estimated with the Chalkley count method under a bright-field microscope. The values represent means of capillary tube score + S.D. based on three wells/data point in a single experiment. *, significantly different from control at $p < 0.05$.

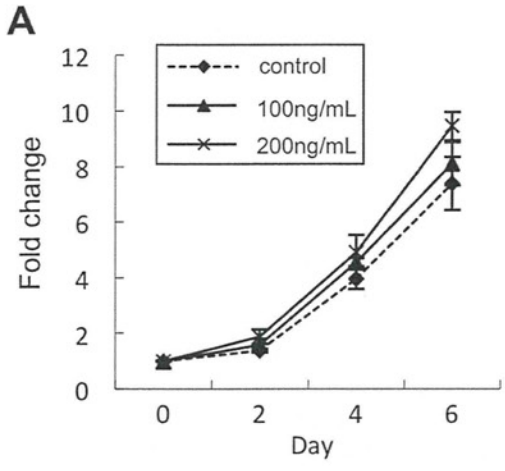

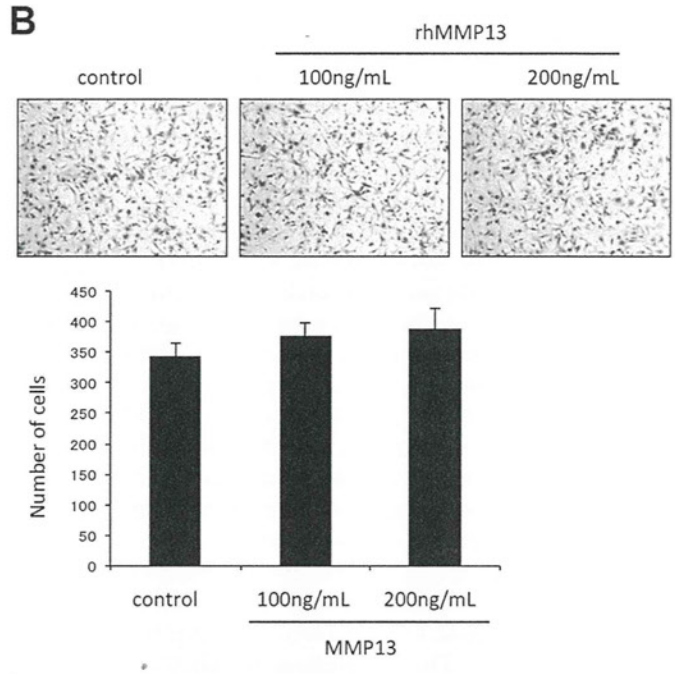

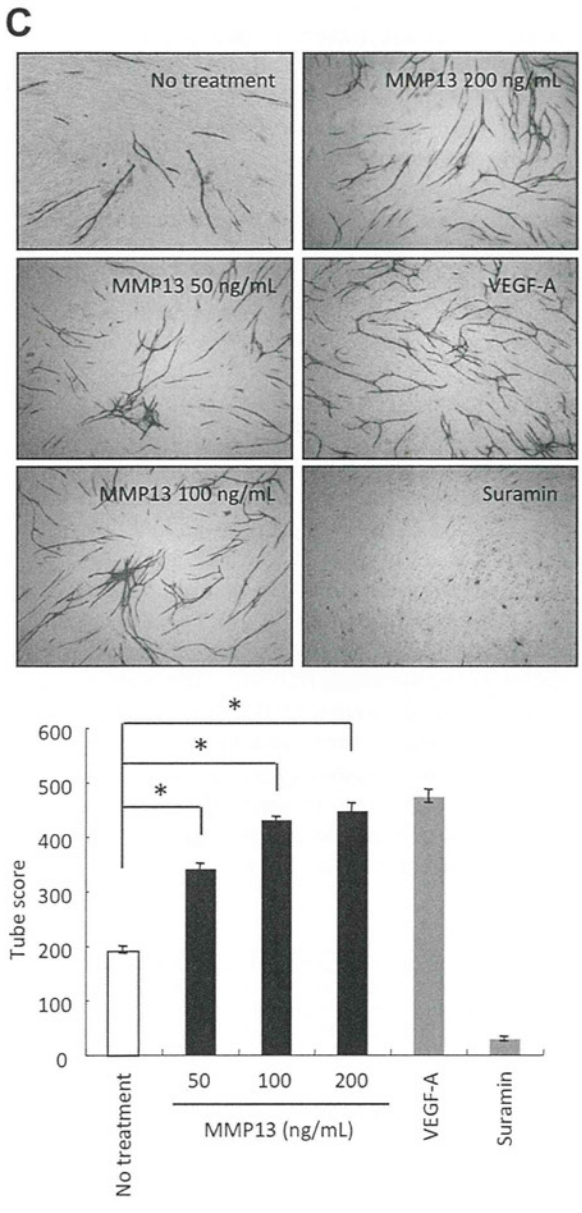

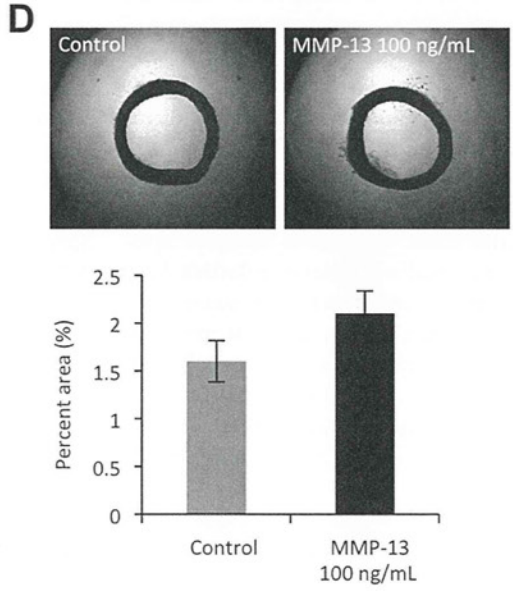

methanol containing 0.3% H_2O_2 for 30 min. Antigen retrieval was done by the microwaving using a citrate phosphate buffer (pH 6.0), and then the sections were incubated with the primary antibody at 4 °C overnight. Immunohistochemical staining was carried out by a monoclonal anti-MMP-13 antibody (Fuji Company Industries, 1:80). For detection of the reaction after incubation with secondary antibodies, we used diaminobenzidine (DAKO, Glostrup, Denmark). The sections were counterstained by hematoxylin and dehydrated in ascending grades of ethanol, and finally, the slides were mounted. By considering the percentage of positive cells and the overall staining intensity, MMP-13 was considered positive if over 10% of the tumor cells showed strong or diffuse staining. If less than 10% of the cells showed weak or no staining, it was considered negative.

Assay for Blood Vessel Density—CD34 is an antigen present in hematopoietic progenitor cells and endothelial cells. Anti-CD34 antibody is a highly sensitive marker for endothelial cell differentiation and has also been studied as a marker for vascular tumors. To investigate the relation between angiogenesis and MMP-13, we stained all HNSCC cases with CD34 endothelial marker (Novocastra Laboratories Ltd., Newcastle, UK) by SABC method. To assess blood vessel density, we performed histomorphometric analysis. Three representative photomicrographs (areas where MMP-13 positivity were detected including invasive front) were taken from each case stained with CD34. First, we went through all the sections stained with MMP-13 and CD34 antibodies. The area was selected by the following criteria: (i) the expression of MMP-13, (ii) the included invasive tumor front, and (iii) the high number of blood vessels. Photographs of those tumors were taken in close proximity to MMP-13-expressing area including the invasive front. For MMP-13-negative cases, three areas from the invasive front were selected. Any positively stained endothelial cell or endothelial cell cluster, with or without a lumen, was considered as a single, countable blood vessel. Stromal area was quantitatively analyzed using digital image (Adobe Photoshop and Scion Image software). From each figure, total counts of blood vessels per stromal area were taken, and the average was calculated. The results were then compared with MMP-13 expression.

Statistical Analysis—A p value < 0.05 was required for assessing the significance. Correlation between variables was estimated using Fisher's exact test, and for correlation between MMP-13 expression and blood vessel density, a Welch test was used.

RESULTS

MMP-13 Promotes Angiogenesis—We previously identified periostin, interferon-induced transmembrane protein 1 (IFITM1), and Wnt-5b as cancer invasion-related factors by comparing the gene expression profiles between parent and highly invasive clone of a cancer cell line (22). MMP-13 was identified as a common up-regulated molecule by comparing the gene expression profiles between control cells and periostin-overexpressing cells, control cells and IFITM1-overexpressing cells, and control cells and Wnt-5b-overexpressing cells (Fig. 1*A*) (26). It is known that MMP-13 is highly expressed in various tumors and is related to tumor behavior and prognosis (18). To know the role of MMP-13 in cancer development, we generated MMP-13-overexpressing cancer cells. Expression of MMP-13 mRNA was examined in six head and neck cancer cell lines (Fig. 1*B*). Among six cell lines, HSC2 and HSC3 cells showed lower expression of MMP-13 mRNA. Expression level of MMP-13 in these cells was lower than that in other cancer cells. Therefore, we transfected a FLAG-MMP-13 plasmid into HSC3 cells. Then, we obtained four stable clones and one stable pool clone of MMP-13-overexpressing cells (Fig. 1*C*). All stable clones highly expressed ectopic MMP-13 (Fig. 1*C*). In further experiments, clone 1 was used. By using MMP-13-overexpressing cells, we examined the role of MMP-13 in cell growth and invasion. MMP-13 overexpression did not affect cell proliferation and slightly promoted the invasion of HNSCC cells (data not shown). We also confirmed that conditioned medium from MMP-13-overexpressing cells had a higher protease activity than that from control cells (Fig. 1*D*).

MMP-13 has recently been shown to play a critical role in the process of angiogenesis during the healing of fracture (15). Here, we examined the role of MMP-13 in angiogenesis. MMP-13 secretion was detected in conditioned medium from MMP-13-overexpressing-HSC3 cells by Western blot analysis (Fig. 1*E*). Expression level of ectopic MMP-13 in MMP-13-overexpressing HSC3 cells was similar to that of endogenous MMP-13 in Ho-1-N-1 or HSC4 cells (Fig. 1*F*). By using conditioned medium from MMP-13-overexpressing cells, we examined the migration of immortalized HUVECs. The HuhT1 cell line was previously established from HUVECs by transfection with human telomerase reverse transcriptase (20). Conditioned medium from MMP-13-overexpressing cells promoted migration of HuhT1 cells (Fig. 2*A*). Interestingly, conditioned medium from MMP-13-overexpressing cells significantly promoted capillary tube formation, in comparison with that from

FIGURE 3. **MMP-13 promoted angiogenesis both *in vitro* and *in vivo*.** *A*, effect of MMP-13 on the proliferation of HuhT1 cells. Cells were plated on 24-well plates, and trypsinized cells were counted by Cell Counter at 0, 2, 4, and 6 days after adding recombinant MMP-13 protein (100 or 200 ng/ml). *B*, migration activity by recombinant MMP-13 protein. Migration activity was measured as described in Fig. 1*E*. The *upper panel* shows the representative area of penetrated cells. The *lower graph* shows the average number of penetrated cells. The *bars* show the average values and S.D. of three independent experiments. *C*, *upper panel* shows the representative area of capillary tube formation by treatment with recombinant MMP-13 protein (50, 100, and 200 ng/ml) (×40). VEGF-A (2 μg/ml) was used as a positive control, and suramin (1 mM) was used as a negative control. Capillary tube formation was examined as described in Fig. 1*F*. The *lower graph* shows the average capillary tube score after treatment with recombinant MMP-13 protein. The capillary tube score was estimated with the Chalkley count method under a bright-field microscope. The values represent means of capillary tube score + S.D. based on three wells/data point in a single experiment. *, $p < 0.05$. *D*, *upper panel* shows representative case of culturing aortic explants in three-dimensional matrix gels with or without recombinant MMP-13 protein (100 ng/ml). Excited thoracic aorta (1-mm-long cross-sections) was placed on the Matrigel-coated wells and covered with an additional 50 μl of Matrigel. Afterward, Control was treated with EBM-2 medium only or EBM-2 medium containing recombinant MMP-13 protein. Each medium was added every other day. All assays were performed by using five aortic rings per sample. Aortic rings were photographed on day 15. The area of angiogenic sprouting was calculated using Image-Pro Plus software program (Media Cybernetics). The *lower graph* shows microvessel densities in square pixels.

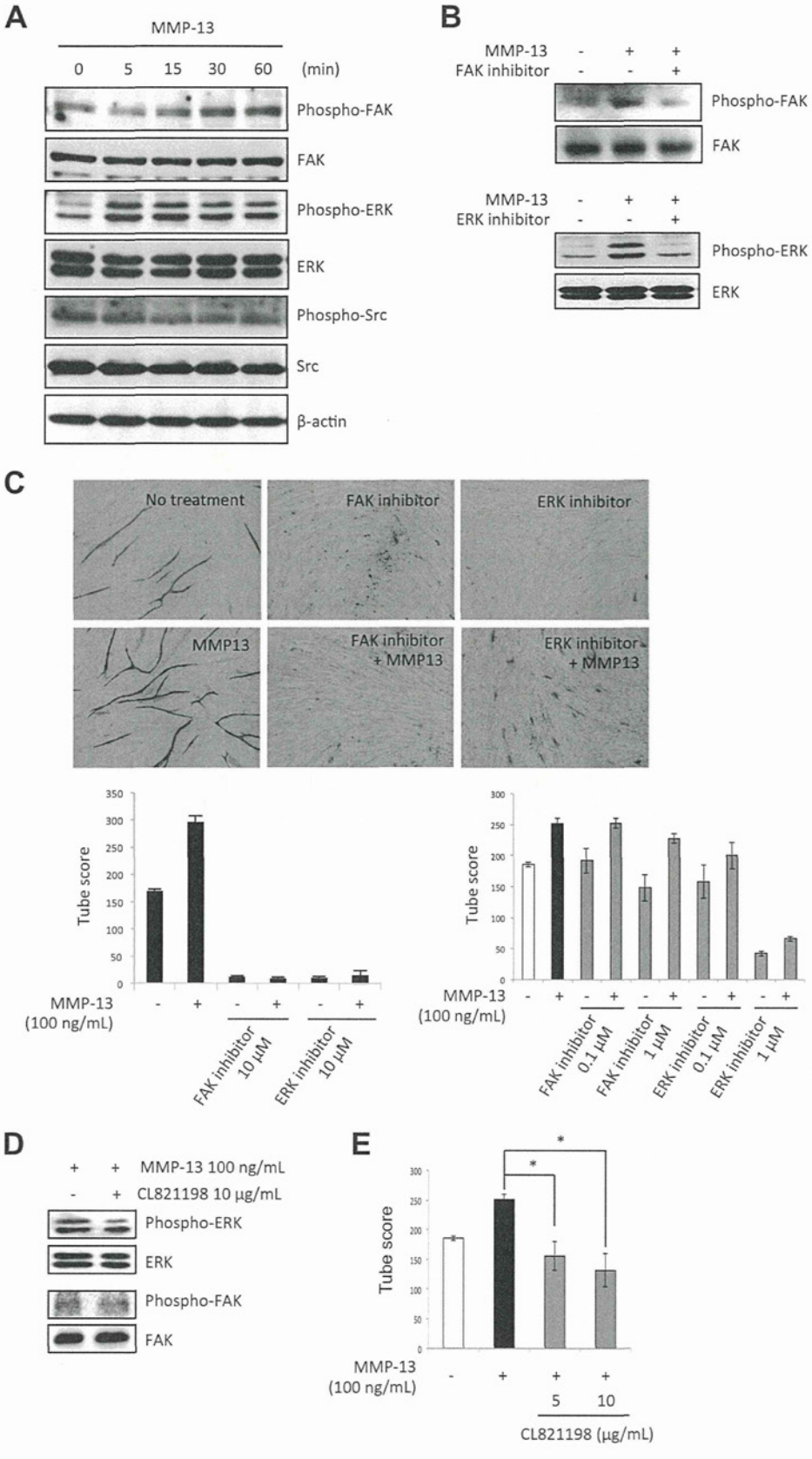

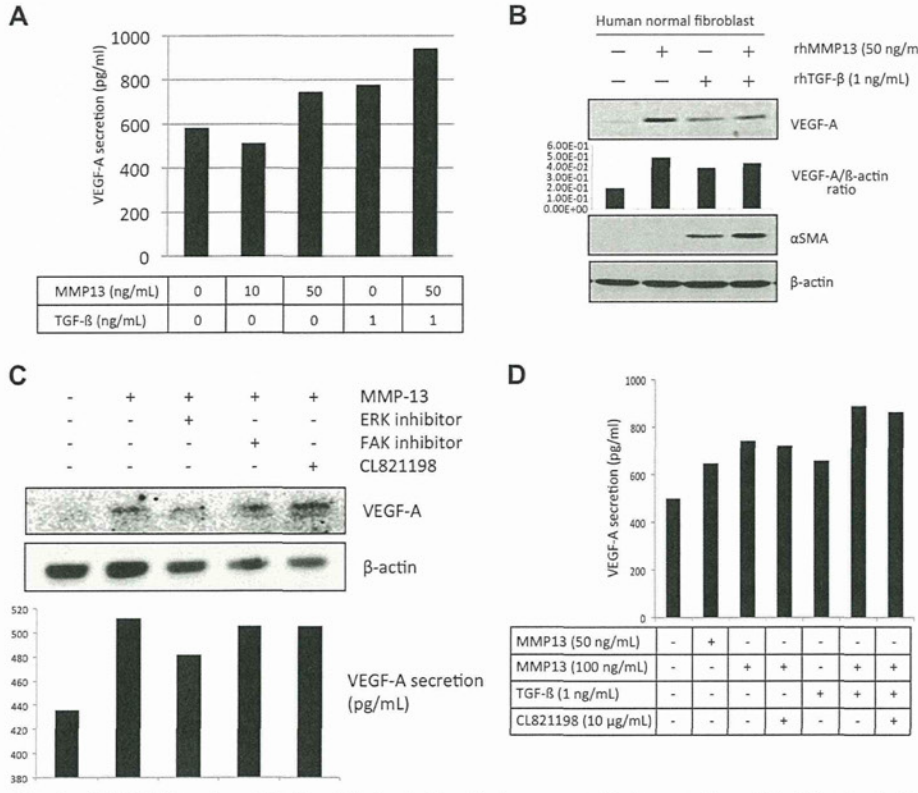

FIGURE 5. **VEGF-A secretion by MMP-13 treatment in fibroblasts.** *A*, fibroblasts were seeded on a culture dish. After incubation for 24 h, medium was changed to DMEM without FBS. After 24 h, MMP-13 (0, 10, and 50 ng/ml) and TGF-β (1 ng/ml) with or without MMP-13 (50 ng/ml) were treated for 24 h. The concentration of VEGF-A in the culture medium was quantified with commercial ELISA kits according to the manufacturer's instructions. *B*, after treatment with MMP-13 (0, 10, and 50 ng/ml) or TGF-β (1 ng/ml) with or without MMP-13 (50 ng/ml) for 24 h, fibroblasts were collected. Expressions of VEGF-A, α-SMA, and β-actin were examined by immunoblotting. The densitometric analysis of VEGF-A expression was performed. VGEF-A/β-actin ratio is shown. *C*, HuhT1 cells were seeded on a culture dish. After incubation for 24 h, medium was changed to HuMedia without FBS and growth factors. After 4 h, the recombinant MMP13 protein (100 ng/ml) with or without 10 μM of FAK inhibitor (FAK inhibitor 14), 10 μM of ERK inhibitor (U0126) or 10 μg/ml of CL-821198 were added and the cells were incubated for 1 h. Expression of VEGF-A and β-actin were examined by immunoblotting. The concentration of VEGF-A in the culture medium was quantified with commercial ELISA kits according to the manufacturer's instructions. *D*, fibroblasts were seeded on a culture dish. After incubation for 24 h, medium was changed to DMEM without FBS. After 24 h, MMP-13 (0, 50, and 100 ng/ml) and TGF-β (1 ng/ml) with or without MMP-13 (100 ng/ml) were treated for 24 h. Moreover, we treated CL-821198 (10 μg/ml). The concentration of VEGF-A in the culture medium was quantified with commercial ELISA kits according to the manufacturer's instructions.

empty vector-transfected HSC3 cells (Fig. 2*B*). Moreover, we examined MMP-13 knockdown in Ho-1-N-1 or HSC4 cells with MMP-13 expression. MMP-13 siRNA reduced MMP-13 expression and protease activity (Fig. 1, *D* and *F*). Conditioned medium from MMP-13-depleted cells suppressed migration and capillary tube formation (Fig. 2, *C* and *D*).

To exclude other factors in conditioned medium, we used recombinant MMP-13 protein for *in vitro* angiogenesis assay. We examined the effect of recombinant MMP-13 protein on cell growth and migration of HuhT1 cells. Treatment with recombinant MMP-13 protein did not significantly promote cell growth and migration of HuhT1 cells (Fig. 3, *A* and *B*). For

FIGURE 4. **MMP-13-promoted angiogenesis is mediated by FAK and ERK signaling pathway.** *A*, levels of total and phosphorylated forms of FAK, Src, and ERK after treatment of HuhT1 cells with MMP-13 (100 ng/ml) shown by Western blotting. β-Actin expression was used as a loading control. HuhT1 cells were seeded on a culture dish. After incubation for 24 h, medium was changed to HuMedia without FBS and growth factors. After 4 h, the recombinant MMP13 protein (100 ng/ml) was added and the cells were incubated for indicated times. *B*, phosphorylated forms of FAK (Tyr-576/577), Src (Tyr-416) and ERK (Thr-202/Tyr-204) in the presence of MMP-13 (100 ng/ml) after treatment with 10 μM FAK inhibitor (FAK inhibitor 14) or 10 μM ERK inhibitor (U0126). Expression of total FAK or ERK was used as a loading control. *C*, *upper panel* shows the representative area of capillary tube formation by FAK inhibitor (FAK inhibitor, 14 or 10 μM) or ERK inhibitor (U0126, 10 μM) with or without MMP-13 (100 ng/ml) ($\times$40). The *lower left graph* shows the average tubule score after 10 μM FAK inhibitor (FAK inhibitor 14) or 10 μM of ERK inhibitor (U0126) with or without 100 ng/ml of recombinant MMP-13 protein. The *lower right graph* shows the average tubule score after FAK inhibitor (0.1 and 1 μM) or ERK inhibitor (0.1 and 1 μM) with or without 100 ng/ml of recombinant MMP-13 protein. The values represent means of capillary tube score + S.D. based on three wells/data point in a single experiment. *D*, to examine the effect of protease inhibition on FAK and ERK phosphorylation, CL-821198, which is a selective inhibitor of MMP-13 through the binding to the S1′ pocket of MMP-13 with its morpholine ring adjacent to the catalytic zinc atom, was used. HuhT1 cells were seeded on a culture dish. After incubation for 24 h, medium was changed to HuMedia without FBS and growth factors. After 4 h, CL-821198 (10 μg/ml) and/or recombinant MMP13 protein (100 ng/ml) were added, and the cells were incubated for 1 h. Levels of total and phosphorylated forms of FAK and ERK was examined by Western blotting. *E*, capillary tube formation was examined by using an angiogenesis assay kit. HUVECs were treated with the recombinant MMP-13 protein with or without CL-821198 (5 and 10 μg/ml), and the medium was changed every 3 days. After 12 days, the cells were fixed and stained with anti-human CD31 antibody. The graph shows the average capillary tube score after treatment with recombinant MMP-13 protein. The capillary tube score was estimated with the Chalkley count method under a bright-field microscope. The values represent means of capillary tube score + S.D. based on three wells/data point in a single experiment. *, $p < 0.05$.

in vitro angiogenesis assay, we used VEGF-A as a positive control and suramin as a negative control. Similarly to conditioned medium from MMP-13-overexpressing cells, treatment with MMP-13 protein significantly promoted capillary tube formation in a concentration-dependent manner (Fig. 3*C*). Surprisingly, capillary tube score of MMP-13 treatment was similar to that of VEGF-A (Fig. 3*C*). However, MMP-13 did not significantly stimulate microvessel outgrowth from aorta comparing with control (Fig. 3*D*).

To clarify the mechanism of MMP-13-promoted angiogenesis, we examined the involvement of several intracellular signaling molecules such as FAK, Src, and ERK by Western blotting using phosphorylation specific antibodies in HuhT1 cells after adding recombinant MMP-13 protein. Increased phosphorylation of FAK and ERK was observed after adding MMP-13 protein (Fig. 4*A*). To demonstrate the involvement of FAK and ERK in MMP-13-promoted angiogenesis, we examined capillary tube formation after treatment with FAK inhibitor (FAK inhibitor 14) or ERK inhibitor (U0126) together with recombinant MMP-13 protein. We confirmed that treatment with FAK inhibitor 14 or U0126 suppressed FAK or ERK activity, respectively (Fig. 4*B*). Both inhibitors inhibited MMP-13-promoted capillary tube formation in a concentration-dependent manner (Fig. 4*C*). Both inhibitors also inhibited capillary tube formation without MMP-13 treatment in a concentration-dependent manner (Fig. 4*C*), suggesting that the FAK and ERK signaling pathway may be a conventional pathway of angiogenesis. Moreover, FAK inhibitor did not influence on ERK activity and ERK inhibitor did not influence on FAK activity in MMP-13-treated endothelial cells (data not shown), suggesting that the inhibitory effects exerted by either FAK or ERK inhibitor are separated. These findings suggest that MMP-13 may promote angiogenesis via a conventional pathway.

To know whether ERK or FAK activity induced by MMP-13 was caused by protease activity of MMP-13, we examined the effect of protease inhibition on FAK and ERK phosphorylation by using CL-821198, which is a selective inhibitor of MMP-13 through the binding to the S1′ pocket of MMP-13 with its morpholine ring adjacent to the catalytic zinc atom. CL-821198 treatment did not influence on ERK or FAK activity in HuhT1 cells (Fig. 4*D*). This finding indicates that ERK or FAK activity induced by MMP-13 is not caused by protease activity of MMP-13. We also examined the effect of CL-821198 on capillary tube formation. CL-821198 inhibited MMP-13-promoted tube formation. This finding suggests that MMP-13 activity may affect to capillary tube formation via an ERK- or FAK-independent manner (Fig. 4*E*).

MMP-13 Promotes VEGF-A Secretion in Fibroblasts and Endothelial Cells—A recent report shows that esophageal squamous cell carcinoma-derived TGF-β regulates angiogenesis through the release of VEGF from fibroblasts (27). We examined whether MMP-13 affected the release of VEGF from fibroblasts or endothelial cells as a similar function of TGF-β. Normal fibroblasts were obtained from gingival tissues using standard explant techniques (21). The level of VEGF-A secretion by fibroblasts was measured after being induced by MMP-13 with/without the presence of TGF-β. Interestingly, MMP-13 could promote the secretion of VEGF-A, especially in the presence of TGF-β (Fig. 5*A*). It is known that paracrine tumor-derived growth factors activate the cancer-associated fibroblasts, which undergo a myofibroblastic transdifferentiation defined by an elongated spindle shape, and the expression of contractile α-SMA and vimentin (28). Therefore, we examined the expression of α-SMA after TGF-β or MMP-13 treatment in fibroblasts. As previously reported, TGF-β induced α-SMA expression in fibroblasts (Fig. 5*B*). Although MMP-13 itself did not induce α-SMA expression in fibroblasts, both TGF-β and MMP-13 induced higher expression of α-SMA in comparison with the expression level of α-SMA induced by TGF-β (Fig. 5*B*).

TABLE 1
Correlation between MMP-13 expression and clinicopathologic findings in HNSCC

		MMP-13 expression		
	No. of cases	Low	High	p value
Non-neoplastic epithelium	30	30 (100%)	0 (0%)	$p < 0.001$
HNSCC	67	13 (19.4%)	54 (80.6%)	
Metastasis				
−	30	7 (23.3%)	23 (76.7%)	
+	37	6 (16.2%)	31 (83.8%)	

Moreover, we examined whether MMP-13-promoted VEGF-A secretion from the endothelial cell line HuhT1 or not. Interestingly, the expression and secretion levels of VEGF-A were increased by MMP-13 treatment (Fig. 5, *C* and *D*). Induction of VEGF-A in HuhT1 cells was partially dependent on ERK activity but not on FAK activity and MMP-13 protease activity (Fig. 5, *C* and *D*).

MMP-13 Is Highly Expressed in Human Cancer Tissues—To demonstrate *in vitro* and *in vivo* evidence of MMP-13-mediated angiogenesis, we examined the expression of MMP-13 and its relationship with tumor angiogenesis in clinical cancer cases. We examined the immunohistochemical expression of MMP-13 in 20 normal oral epithelium and 67 HNSCC tissues. Positive expression of MMP-13 was observed in 0 of 20 (0%) normal oral epithelium and 54 of 67 (81%) HNSCC cases (Fig. 5, *A* and *B*, and Table 1). We compared MMP13 expression with metastasis in HNSCC cases. MMP-13 expression was well correlated with metastasis (Table 1). Then, we compared MMP-13 expression with the number of blood vessels in HNSCC cases. The number of blood vessels was examined by staining using anti-CD34 antibody. CD34 is an antigen present in hematopoietic progenitor cells and endothelial cells. Anti-CD34 antibody is a highly sensitive marker for endothelial cell differentiation and has also been studied as a marker for vascular tumors. We observed an increased number of blood vessels at the invasive front of the MMP-13 positive tumor cases, compared with the MMP-13 negative cases ($p < 0.05$) (Fig. 6, *A* and *B*). The average number of blood vessel density assessed by histo-morphometric analysis was 41.4 ± 13.0 and 76.2 ± 26.6 in MMP-13 negative and positive cases, respectively ($p < 0.05$) (Fig. 6*C* and Table 1).

DISCUSSION

Angiogenesis, the formation of new blood vessels from preexisting ones, is a crucial step in tumor growth, progression, and metastasis. Regulation of angiogenesis *in vivo* is complex and is controlled by a variety of factors. Among them, VEGF is considered to play a dominant role. It has been well established that VEGF promotes a cancer progression by up-regulating

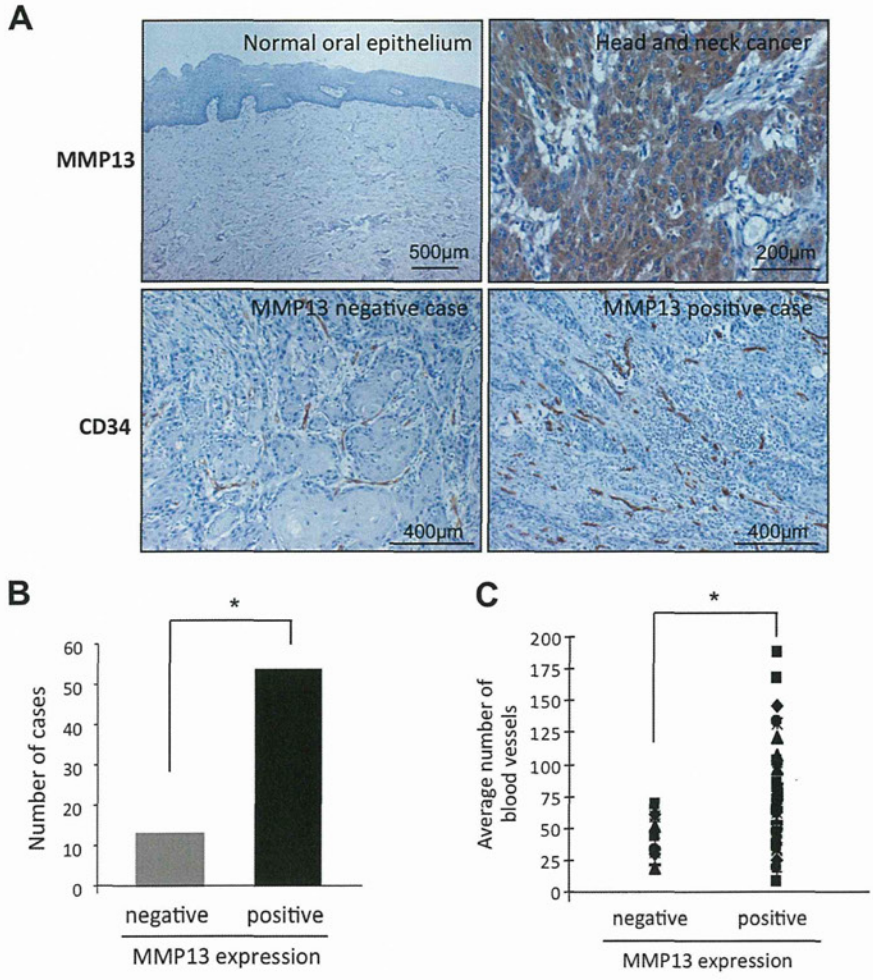

FIGURE 6. **MMP-13 expression is well correlated with the number of blood vessels in human cancer cases.** *A*, immunohistochemical staining of MMP-13 and CD34 in normal oral epithelium and HNSCC. Representative cases of MMP-13 expression in normal oral epithelium and HNSCC are shown. Representative cases of CD34 expression in HNSCC cases with or without MMP-13 expression are also shown. *B*, graph shows the number of cases with or without MMP-13 expression in 67 HNSCC cases. *, $p < 0.05$. *C*, graph shows the average number of blood vessels in HNSCC cases with or without MMP-13 expression. *, $p < 0.05$.

microvessel density (3). MMPs are zinc metalloenzymes with the ability to degrade the components of the ECM. Their action is crucial during the progression of cancer because they allow the remodeling of the surrounding healthy tissues and enable local invasion (8). MMP-13 is known as collagenase-3, which has the ability to degrade fibrillar collagen (29). However, it may also act as a potent gelatinase by degrading a wide variety of extracellular matrix components (30, 31). MMP-13 is overexpressed in a variety of tumors from such as head and neck, laryngeal, breast, chondrosarcoma, gastric, colorectal, vulvar carcinomas and cutaneous malignant lymphoma (17, 32–39). In most malignancies, MMP-13 has been correlated with tumor invasion, metastasis, and poor prognosis in patients (34, 35, 37, 39, 41). MMP-13 is predominantly expressed by tumor cells at the tumor invasive front and to some extent by stromal fibroblasts surrounding tumor cells (33, 41). Our immunohistochemical finding that MMP-13 expression is frequently observed, but no statistical correlation was observed in MMP-13 expression and metastasis in HNSCC (Table 1). As we used biopsy cases in this study, HNSCC cases with high expression of MMP-13 may have a potential to metastasize later. Indeed, MMP-13 expression was well correlated with number of blood vessels. Thus, it is well accepted that MMP-13 is involved in tumor progression.

In the present study, we demonstrate the novel role of MMP-13 in tumor angiogenesis. Although there is a study suggesting a role of MMP-13 in keratinocyte migration and angiogenesis during the healing of fracture (43), the role of MMP-13 in tumor angiogenesis has not been fully elucidated. It is known that some MMPs such as MMP-1, -2, -3, -7, -9, -14 and -16 are involved in tumor angiogenesis via the regulation of bioavailability of VEGF-A (11). Distinct from the function of other MMPs in angiogenesis, MMP-13 promoted angiogenesis through an increased number of blood vessels at the invasive front of the tumor and up-regulation of VEGF-A secretion from fibroblasts and endothelial cells (Fig. 7). We also found that MMP-13 promoted capillary tube formation was mediated by activation of FAK and ERK. FAK is a cytoplasmic tyrosine kinase that plays critical roles in integrin-mediated signal transductions and also participates in signaling by other cell surface receptors (44). Extensive studies in FAK knock-out mouse models indicated a critical role of FAK in angiogenesis during

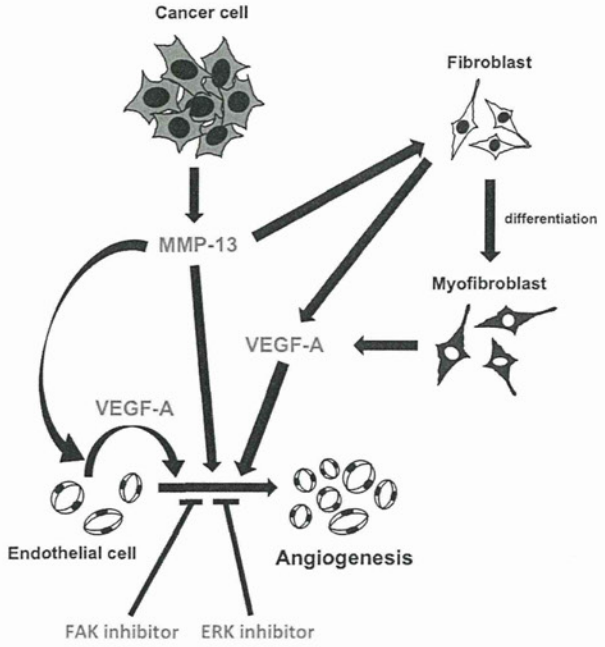

FIGURE 7. **A model of MMP-13-promoted angiogenesis.** MMP-13 is secreted from cancer cells. MMP-13 promotes angiogenesis through FAK and ERK signaling pathway. Moreover, MMP-13 enhances the secretion of VEGF-A from endothelial cells, fibroblasts or myofibroblasts. Secreted VEGF-A promotes angiogenesis.

embryonic development (45). Moreover, the increased expression of FAK in cancer cells has been suggested to play a role in the tumor angiogenic switch to promote aggressive tumor progression and metastasis (46). However, Baek *et al.* (47) found that the MEK/ERK pathway is involved in endothelial cell proliferation through up-regulation of positive cell cycle proteins and down-regulation of negative cell cycle proteins. Thus, activation of FAK and ERK is critically involved in angiogenesis. Indeed, treatment with FAK inhibitor or ERK inhibitor strongly inhibited the capillary tube formation of endothelial cells, suggesting that FAK and ERK signaling are essential in angiogenesis. Although MMP-13 has central roles in modulating extracellular matrix degradation through its direct matrix degrading capability as well as having a key involvement in the activation of other MMPs (7), FAK or ERK activity induced by MMP-13 was not mediated by matrix degrading capability (Fig. 4*D*). Our findings suggest that MMP-13-driven angiogenesis may be mediated by a conventional pathway via activation of FAK and ERK. However, the mechanism of ERK or FAK activation by MMP-13 is still unclear.

The tumor tissue consists of a dynamic mixture of tumor cells, fibroblasts, endothelial cells, and immune cells that all work together to drive tumor progression (48). Activated fibroblasts, also known as cancer-associated fibroblasts within the tumor microenvironment, is preceded by the chemoattraction and migration of precursor cells, which can either arise from the surrounding host fibroblasts or from circulating mesenchymal precursor cells (40, 42, 49). Cancer-associated fibroblasts are activated by paracrine tumor-derived growth factors, which undergo a myofibroblastic transdifferentiation (28). Noma *et al.* (27) showed that paracrine TGF-β from the esophageal cancer cells lead to activation of the fibroblasts and vascular network formation through the release of VEGF-A. Interestingly, MMP-13 induced the secretion of VEGF-A from fibroblasts in similar to TGF-β. Moreover, TGF-β induced α-SMA expression in fibroblasts, indicating that the phenotypic switch from fibroblast to myofibroblast may be caused by TGF-β. MMP-13 itself could not induce α-SMA expression, but it enhanced α-SMA expression induced by TGF-β. Although TGF-β induced a myofibroblastic transdifferentiation of fibroblasts and VEGF-A secretion from myofibroblasts, TGF-β itself inhibited capillary tube formation of endothelial cells (data not shown). Previous report shows MMP-13 increases the expression of VEGF and its receptor, VEGFR-2 (19). In this study, we could not detect VEGFR-2 expression in fibroblasts after treatment with MMP-13 and/or TGF-β by real-time PCR analysis (data not shown). In addition, VEGF-A induction by MMP-13 in fibroblasts and endothelial cells was not dependent on MMP-13 protease activity (Fig. 5, *C* and *D*). Although it is unclear how MMP-13 promotes VEGF-A secretion from fibroblasts and endothelial cells, it is interesting to examine the detailed role of MMP-13 in the tumor microenvironment.

In summary, our findings suggest that MMP-13 may directly and indirectly promote tumor angiogenesis. In various tumors, MMP-13 is correlated with tumor invasion, metastasis, and poor prognosis. Therefore, we believe that MMP-13 can be a potential target for therapeutic intervention to additionally obstruct tumor angiogenesis in cancer patients.

Acknowledgments—The authors thank Dr. Michael Byrne (Harvard Medical School) for providing materials and Dr. Kyoko Hida (Hokkaido University) for discussion. We thank Satoko Katada (Tokushima University), Minori Manabe (Hiroshima University), and Mayumi Ohira (Hiroshima University) for technical assistance.

REFERENCES

1. Fidler, I. J. (1990) Critical factors in the biology of human cancer metastasis: twenty-eighth G.H.A. Clowes memorial award lecture. *Cancer Res.* **50,** 6130–6138
2. Howell, G. M., and Grandis, J. R. (2005) Molecular mediators of metastasis in head and neck squamous cell carcinoma. *Head Neck* **27,** 710–717
3. Folkman, J. (2000) Tumor angiogenesis in *Cancer Medicine* (Holland, J. F., ed) 5th Ed., pp. 132–152, B. C. Decker, Inc., Ontario, Canada
4. Hanahan, D., and Weinberg, R. A. (2000) The hallmarks of cancer. *Cell* **100,** 57–70
5. Bouck, N., Stellmach, V., and Hsu, S. C. (1996) How tumors become angiogenic. *Adv. Cancer Res.* **69,** 135–174
6. Fukumura, D., Xavier, R., Sugiura, T., Chen, Y., Park, E. C., Lu, N., Selig, M., Nielsen, G., Taksir, T., Jain, R. K., and Seed, B. (1998) Tumor induction of VEGF promoter activity in stromal cells. *Cell* **94,** 715–725
7. Egeblad, M., and Werb, Z. (2002) New functions for the matrix metalloproteinases in cancer progression. *Nat. Rev. Cancer* **2,** 161–174
8. Milner, J. M., and Cawston, T. E. (2005) Matrix metalloproteinase knockout studies and the potential use of matrix metalloproteinase inhibitors in the rheumatic diseases. *Curr. Drug Targets Inflamm. Allergy* **4,** 363–375
9. Werner, J. A., Rathcke, I. O., and Mandic, R. (2002) The role of matrix metalloproteinases in squamous cell carcinomas of the head and neck. *Clin. Exp. Metastasis* **19,** 275–282
10. Coussens, L. M., Fingleton, B., and Matrisian, L. M. (2002) Matrix metalloproteinase inhibitors and cancer: trials and tribulations. *Science* **295,** 2387–2392
11. Littlepage, L. E., Sternlicht, M. D., Rougier, N., Phillips, J., Gallo, E., Yu, Y., Williams, K., Brenot, A., Gordon, J. I., and Werb, Z. (2010) Matrix metalloproteinases contribute distinct roles in neuroendocrine prostate carcinogenesis, metastasis, and angiogenesis progression. *Cancer Res.* **70,** 2224–2234

12. Bergers, G., Brekken, R., McMahon, G., Vu, T. H., Itoh, T., Tamaki, K., Tanzawa, K., Thorpe, P., Itohara S., Werb, Z., and Hanahan, D. (2000) Matrix metalloproteinase-9 triggers the angiogenic switch during carcinogenesis. *Nat. Cell Biol.* **2,** 737–744
13. Lee, S., Jilani, S. M., Nikolova, G. V., Carpizo D., and Iruela-Arispe, M. L. (2005) Processing of VEGF-A by matrix metalloproteinases regulates bioavailability and vascular patterning in tumors. *J. Cell Biol.* **169,** 681–691
14. Ribatti, D. (2009) Endogenous inhibitors of angiogenesis: a historical review. *Leuk. Res.* **33,** 638–644
15. Kosaki, N., Takaishi, H., Kamekura, S., Kimura, T., Okada, Y., Minqi, L., Amizuka, N., Chung, U. I., Nakamura, K., Kawaguchi, H., Toyama, Y., and D'Armiento, J. (2007) Impaired bone fracture healing in matrix metalloproteinase-13 deficient mice. *Biochem. Biophys. Res. Commun.* **354,** 846–851
16. Zijlstra, A., Aimes, R. T., Zhu, D., Regazzoni, K., Kupriyanova, T., Seandel, M., Deryugina, E. I., and Quigley, J. P. (2004) Collagenolysis-dependent angiogenesis mediated by matrix metalloproteinase-13 (collagenase-3). *J. Biol. Chem.* **279,** 27633–27645
17. Freije, J. M., Díez-Itza, I., Balbín, M., Sánchez, L. M., Blasco, R., Tolivia, J., and López-Otín, C. (1994) Molecular cloning and expression of collagenase-3, a novel human matrix metalloproteinase produced by breast carcinomas. *J. Biol. Chem.* **269,** 16766–16773
18. Nielsen, B. S., Rank, F., López, J. M., Balbin, M., Vizoso, F., Lund, L. R., Danø, K., and López-Otín, C. (2001) Collagenase-3 expression in breast myofibroblasts as a molecular marker of transition of ductal carcinoma in situ lesions to invasive ductal carcinomas. *Cancer Res.* **61,** 7091–7100
19. Lederle, W., Hartenstein, B., Meides, A., Kunzelmann, H., Werb, Z., Angel, P., and Mueller, M. M. (2010) MMP13 as a stromal mediator in controlling persistent angiogenesis in skin carcinoma. *Carcinogenesis* **31,** 1175–1184
20. Anno, K., Hayashi, A., Takahashi, T., Mitsui, Y., Ide, T., and Tahara, H. (2007) Telomerase activation induces elongation of the telomeric single-stranded overhang, but does not prevent chromosome aberrations in human vascular endothelial cells. *Biochem. Biophys. Res. Commun.* **353,** 926–932
21. Schor, S. L., Schor, A. M., Rushton, G., and Smith, L. (1985) Adult, foetal and transformed fibroblasts display different migratory phenotypes on collagen gels: evidence for an isoformic transition during foetal development. *J. Cell Sci.* **73,** 221–234
22. Kudo, Y., Ogawa, I., Kitajima, S., Kitagawa, M., Kawai, H., Gaffney, P. M., Miyauchi, M., and Takata, T. (2006) Periostin promotes invasion and anchorage-independent growth in the metastatic process of head and neck cancer. *Cancer Res.* **66,** 6928–6935
23. Bishop, E. T., Bell, G. T., Bloor, S., Broom, I. J., Hendry, N. F., and Wheatley, D. N. (1999) An *in vitro* model of angiogenesis: basic features. *Angiogenesis* **3,** 335–344
24. Fox, S. B., Leek, R. D., Weekes, M. P., Whitehouse, R. M., Gatter, K. C., and Harris, A. L. (1995) Quantitation and prognostic value of breast cancer angiogenesis: comparison of microvessel density, Chalkley count, and computer image analysis. *J. Pathol.* **177,** 275–283
25. Bauer, K. S., Cude, K. J., Dixon, S. C., Kruger, E. A., and Figg, W. D. (2000) Carboxyamido-triazole inhibits angiogenesis by blocking the calcium-mediated nitric-oxide synthase-vascular endothelial growth factor pathway. *J. Pharmacol. Exp. Ther.* **292,** 31–37
26. Deraz, E. M., Kudo, Y., Yoshida, M., Obayashi, M., Tsunematsu, T., Tani, H., Siriwardena, S. B., Keikhaee, M. R., Kiekhaee, M. R., Qi, G., Iizuka, S., Ogawa, I., Campisi, G., Lo Muzio, L., Abiko, Y., Kikuchi, A., and Takata, T. (2011) MMP-10/stromelysin-2 promotes invasion of head and neck cancer. *PLoS One* **6,** e25438
27. Noma, K., Smalley, K. S., Lioni, M., Naomoto, Y., Tanaka, N., El-Deiry, W., King, A. J., Nakagawa, H., and Herlyn, M. (2008) The essential role of fibroblasts in esophageal squamous cell carcinoma-induced angiogenesis. *Gastroenterology* **134,** 1981–1993
28. Sappino, A. P., Skalli, O., Jackson, B., Schürch, W., and Gabbiani, G. (1988) Smooth-muscle differentiation in stromal cells of malignant and non-malignant breast tissues. *Int. J. Cancer* **41,** 707–712
29. Uitto, V. J., Airola, K., Vaalamo, M., Johansson, N., Putnins, E. E., Firth, J. D., Salonen, J., López-Otín, C., Saarialho-Kere, U., and Kähäri, V. M. (1998) Collagenase-3 (matrix metalloproteinase-13) expression is induced in oral mucosal epithelium during chronic inflammation. *Am. J. Pathol.* **152,** 1489–1499
30. Tardif, G., Reboul, P., Pelletier, J. P., and Martel-Pelletier, J. (2004) Ten years in the life of an enzyme: the story of the human MMP-13) collagenase-3. *Mod. Rheumatol.* **14,** 1489–1499
31. Ashworth, J. L., Murphy, G., Rock, M. J., Sherratt, M. J., Shapiro, S. D., Shuttleworth, C. A., and Kielty, C. M. (1999) Fibrillin degradation by matrix metalloproteinases: implications for connective tissue remodeling. *Biochem. J.* **340,** 171–181
32. Culhaci, N., Metin, K., Copcu, E., and Dikicioglu, E. (2004) Elevated expression in MMP-13 and TIMP-1 in head and neck squamous cell carcinomas may reflect increased tumor invasiveness. *BMC Cancer* **4,** 1–8
33. Johansson, N., Vaalamo, M., Grénman, S., Hietanen, S., Klemi, P., Saarialho-Kere, U., and Kähäri, V. M. (1999) Collagenase-3 (MMP-13) is expressed by tumor cells in invasive vulvar squamous cell carcinomas. *Am. J. Pathol.* **154,** 469–480
34. Pendás, A. M., Uría, J. A., Jiménez, M. G., Balbín, M., Freije, J. P., and López-Otín, C. (2000) An overview of collagenase-3 expression in malignant tumors and analysis of its potential value as a target in antitumor therapies. *Clin. Chim. Acta* **291,** 137–155
35. Krecicki, T., Fraczek, M., Jelen, M., Podhorska, M., Szkudlarek, T., Zatonski, T. (2003) Expression of collagenase-1 (MMP-1), collagenase-3 (MMP-13) and tissue inhibitor of matrix metalloproteinase-1 (TIMP-1) in laryngeal squamous cell carcinomas. *Eur. Arch Otorhinolaryngol.* **260,** 494–497
36. del Casar Lizcano, J. M., Vizoso Piñeiro, F., González Sánchez, L. O., Martin Suarez, A., Gava, A., Cuesta Fernandez, E., and Diez Santisteban, M. C. (2003) Expression and clinical significance of collagenase-3 (MMP-13) in gastric cancer. *Gastroenterol. Hepatol.* **26,** 1–7
37. Roeb, E., Arndt, M., Jansen, B., Schumpelick, V., and Matern, S. (2004) Simultaneous determination of matrix metalloproteinase (MMP)-7, MMP-1, -3, and -13 gene expression by multiplex PCR in colorectal carcinomas. *Int. J. Colorectal. Dis.* **19,** 518–524
38. Corte, M. D., Gonzalez, L. O., Corte, M. G., Quintela, I., Pidal, I., Bongera, M., and Vizoso, F. (2005) Collagenase-3 (MMP-13) expression in cutaneous malignant melanoma. *Int. J. Biol. Markers* **20,** 242–248
39. Luukkaa, M., Vihinen, P., Kronqvist, P., Vahlberg, T., Pyrhönen, S., Kähäri, V. M., and Grénman, R. (2006) Association between high collagenase-3 expression levels and poor prognosis in patients with head and neck cancer. *Head Neck* **28,** 225–234
40. De Wever, O., and Mareel, M. (2003) Role of tissue stroma in cancer cell invasion. *J. Pathol.* **200,** 429–447
41. Johansson, N., Airola, K., Grénman, R., Kariniemi, A. L., Saarialho-Kere, U., and Kähäri, V. M. (1997) Expression of collagenase-3 (matrix metalloproteinase-13) in squamous cell carcinomas of the head and neck. *Am. J. Pathol.* **151,** 499–508
42. Direkze, N. C., Hodivala-Dilke, K., Jeffery, R., Hunt, T., Poulsom, R., Oukrif, D., Alison, M. R., and Wright, N. A. (2004) Bone marrow contribution to tumor-associated myofibroblasts and fibroblasts. *Cancer Res.* **64,** 8492–8495
43. Hattori, N., Mochizuki, S., Kishi, K., Nakajima, T., Takaishi, H., D'Armiento, J., and Okada, Y. (2009) MMP-13 plays a role in keratinocyte migration, angiogenesis, and contraction in mouse skin wound healing. *Am. J. Pathol.* **175,** 533–546
44. Zhao, X., and Guan, J. L. (2011) Focal adhesion kinase and its signaling pathways in cell migration and angiogenesis. *Adv. Drug Deliv. Rev.* **63,** 610–615
45. Ilić, D., Furuta, Y., Kanazawa, S., Takeda, N., Sobue, K., Nakatsuji, N., Nomura, S., Fujimoto, J., Okada, M., and Yamamoto, T. (1995) Reduced cell motility and enhanced focal adhesion contact formation in cells from FAK-deficient mice. *Nature* **377,** 539–544
46. Gabarra-Niecko, V., Schaller, M. D., and Dunty, J. M. (2003) FAK regulates biological processes important for the pathogenesis of cancer. *Cancer Metastasis Rev.* **22,** 359–374
47. Baek, Y. Y., Cho, D. H., Choe, J., Lee, H., Jeoung, D., Ha, K. S., Won, M. H., Kwon, Y. G., and Kim, Y. M. (2011) Extracellular taurine induces angiogenesis by activating ERK-, Akt-, and FAK-dependent signal pathways. *Eur. J. Pharmacol.* **674,** 629–640
48. Bissell, M. J., and Radisky, D. (2001) Putting tumors in context. *Nat. Rev. Cancer* **1,** 46–54
49. Dvorak, H. F. (1986) Tumors: wounds that do not heal. Similarities between tumor stroma generation and wound healing. *N. Engl. J. Med.* **315,** 1650–1659

ARTICLE IN PRESS

ADR-12337; No of Pages 8

Advanced Drug Delivery Reviews xxx (2012) xxx–xxx

Contents lists available at SciVerse ScienceDirect

Advanced Drug Delivery Reviews

journal homepage: www.elsevier.com/locate/addr

The role of exosomes and microRNAs in senescence and aging☆

Dan Xu [a,b], Hidetoshi Tahara [b,*]

[a] Institute of Environmental Systems Biology, Dalian Maritime University, 1 Linghai Road, Dalian, 116026, P.R. China
[b] Department of Cellular and Molecular Biology, Graduate School of Biomedical Science, Hiroshima University, 1-2-3 Kasumi, Minami-ku, Hiroshima 734–8553, Japan

ARTICLE INFO

Article history:
Received 16 February 2012
Accepted 8 July 2012
Available online xxxx

Keywords:
Exosome
Aging
Senescence
MicroRNA
Tumor suppression
Age-associated disease

ABSTRACT

Senescence is viewed as a cellular counterpart to aging of tissues and organisms, characterized by an irreversible growth arrest and a combination of changes in cell morphology, function and behavior. microRNAs (miRNAs), the most studied small non-coding RNAs, play an important role in many biological processes by the regulation of gene expression. Recent evidence has shown that miRNAs are contained in exosomes that are tiny vesicles of endocytic origin and released by a variety of different cells as a means for cell-to-cell contact and information transfer. Exosomes and miRNAs have been found to participate in the complex networks of cellular senescence and contribute to aging. Here, we will give an overview on the involvement of secretory factors including exosomes and miRNA in the regulation of cellular senescence, demonstrating the potential role of exosomes and miRNAs in biological processes and signaling pathways of senescence and aging.

Contents

1. Introduction

Exosomes are specialized membranous vesicles (40–100 nm in diameter) of endocytic origin. It was first described and observed by tracking the fate of recycling transferrin receptor during maturation of sheep reticulocytes. Exosomes are formed intracellularly via endocytic invagination and are generated by the outward budding at the limiting endosomal membrane of the multivesicular bodies (MVBs), sharing the biochemical characteristics with the internal vesicles of MVBs [1,2]. Exosomes are released into the extracellular environment from a variety of cells, such as, but not limited to, tumor cells, dendritic cells, lymphoid cells, mesothelial cells, epithelial cells, or cells from different tissues or organs. Thus, cells may communicate through membrane transfer by the secretion of exosomes [3]. Exosomes contain proteins, mRNAs, miRNAs, and signaling molecules that reflect the physiological state of their cells of origin and consequently provide a rich source of potential biomarker molecules [4,5]. Recently, exosomes have been recognized that they appear as a vectorized signaling system operating from inside a donor cell towards either the periphery, the cytosol, or possibly to the nucleus of target cells. Exosomes have been detected to date in various body fluids such as urine, serum, saliva and breast milk, function in intercellular communication, immune system modulation and tumor progression [6–8].

In the past few years, the importance of miRNAs, an abundant class of small non-coding RNAs, has rapidly emerged as important contributors to gene regulation. miRNAs form a particular class of 21- to 24-nucleotide RNAs that can regulate gene expression post-transcriptionally by affecting the translation and stability of target messenger RNAs (mRNAs). Due to the multiple target genes regulated by one miRNA, miRNAs resemble an

☆ This review is part of the *Advanced Drug Delivery Reviews* theme issue on "Exosomes: a key to delivering genetic materials."

* Corresponding author.
E-mail address: toshi@hiroshima-u.ac.jp (H. Tahara).

0169-409X/$ – see front matter © 2012 Elsevier B.V. All rights reserved.
doi:10.1016/j.addr.2012.07.010

Please cite this article as: D. Xu, H. Tahara, The role of exosomes and microRNAs in senescence and aging, Adv. Drug Deliv. Rev. (2012), doi:10.1016/j.addr.2012.07.010

additional layer of complexity to gene regulation and influence global cellular responses ranging from cell cycle regulation, cell proliferation, apoptosis, to development and differentiation [9,10]. They have been shown to have unique tissue-specific, developmental stage-specific or disease-specific patterns, which were reflected by miRNA expression profiles and specific miRNA functions.

In the most recent years, the relevance of exosomes and miRNAs in many fields has been recognized. Circulating miRNAs have been thought to be a new potential biomarker for cancer diagnosis and prognosis [11]. They are strikingly stable in blood plasma/serum and cell culture media, which might be associated with exosomes that contain miRNAs and therefore protect miRNAs against RNase activity [3,12]. Exosome-mediated miRNA transfer is an important mechanism of intercellular communication [13]. It is reported that let-7 miRNA family could be selectively secreted into the extracellular environment via exosomes in a metastatic gastric cancer cell line, implying the involvement of exosomes in miRNA-regulated tumorigenesis [14].

In regard to senescence, some miRNAs have emerged as key regulators during cellular senescence [15–18]. Recently, it has been reported that senescence is associated with the release of exosomes, and senescence-associated exosomes can transfer cargos between cells to mediate cell–cell communication during cellular senescence [19]. In this review, we will focus on recent advances in understanding the diverse regulatory role of exosomes and miRNAs on senescence and aging.

2. Cellular senescence and signaling pathway of senescence

Cellular senescence is a permanent state of growth arrest, accompanied by altered cell physiology and behaviors. It was first described as a limit to the replicative life span of somatic cells. This type of senescence is called replicative senescence, which is triggered by telomere attrition after serial cultivation in vitro [20]. Cellular senescence is also caused prematurely by intrinsic- and/or extrinsic-stress factors including DNA damage, reactive oxygen species and activated oncogene expression [21], sharing similar apparent senescence phenotypes with replicative senescence. Senescent cells exhibit an enlarged and flattened morphology, distinctive nuclear structure of heterochromatin, induction of SA-β-galactosidase activity and altered gene expression [22,23].

Cellular senescence is mainly controlled by the p53–p21 and p16–pRB tumor suppression pathways. The p53 pathway is regulated at multiple points by proteins such as the E3 ubiquitin-protein ligase HDM2 (MDM2 in mice), which facilitates p53 degradation; alternate-reading-frame protein (ARF), which inhibits HDM2 activity; and Sirtuin 1 (SIRT1), which interacts with p53 and deacetylates the Lys382 residue of p53, thereby decreasing p53-mediated transcriptional activation [24,25]. p21 is a crucial transcriptional target of p53 and downstream mediator of p53-dependent senescence [26]. Moreover, p21 itself also mediates a transient DNA damage induced growth arrest and Ras-induced senescence [27]. Senescence signals that engage the p16–pRB pathway generally do so by inducing the expression of p16 that prevents pRB phosphorylation and inactivation. pRB halts cell proliferation by suppressing the activity of E2F, a transcription factor that stimulates the expression of genes that are required for cell cycle progression. E2F can also induce ARF expression, which engages the p53 pathway. So, there is reciprocal regulation between the p53–p21 and p16–pRB pathways. Senescence-inducing signals, including DNA damage, oncogenic stresses as well as oxidative stress, usually engage the p53 and/or the pRB pathways [21]. However, there are differences in how cells respond when one or the other pathway mediates a senescence response. In addition, RAF-induced senescence independent of both p53 and pRB has been reported in human cells [28].

Considering the importance of a family of protein kinases known as cyclin-dependent kinases (CDKs) and CDK inhibitors (CKIs) in controlling cell cycle progression, their activity is of special relevance to senescence. The activity of the CDK4–6/D kinases is followed by the subsequent activation of the CDK2/cyclin E and CDK2/cyclin A kinases, which in turn trigger DNA replication. CKIs fall into two families: the INK4 family and the Cip/Kip family. The INK4-type CKIs such as p16 specifically associate and inhibit the CDK4-6 kinases. The Cip/Kip proteins including p21, p27 and p57 associate to both CDK4-6/D and CDK2/E-A kinases with dramatically different effects, depending on the relative abundance of the different CDK complexes [29]. Overexpression of CDK4 and CDK6 extends the lifespan of human fibroblasts, suggesting that these factors are key regulator of cellular senescence [30]. It is reported that there were differential roles for p21 and p16 in the mechanisms of senescence in human fibroblasts [31]. Up-regulation of p16 may be essential for maintenance of the senescent cell cycle arrest, whereas p21 may be responsible for inactivation of both cyclin E- and cyclin D1-associated kinase activity at the early stage of senescence.

Recent studies about INK4-ARF locus link epigenetics to senescence pathway [32]. Transcriptional regulation of the INK4-ARF locus plays the pivotal role in senescence, placing chromatin regulation as a critical pathway in senescence. Epigenetic repression of INK4-ARF is controlled by a crosstalk of several chromatin modulators. The polycomb group (PcG) proteins are direct regulators of the INK4-ARF locus, which catalyze histone modifications that promote changes in chromatin structure. Overexpression of the PcG proteins CBX8 delays the onset of replicative senescence in human cells [33]. DNA methyltransferases (DNMTs) and histone deacetylases (HDACs) are also epigenetic regulators of the INK4-ARF locus. Overexpressed DNMTs in cancer cells lead to aberrant hypermethylation, which impairs expression of tumor suppressor genes by methylation of the CpG islands within promoter regions [34]. The promoters of p16 and p21 are found to be hypermethylated and therefore repressed in various cancer cell lines [35,36], suggesting that DNA methylation may be involved in cellular senescence. Modulation of histone acetylation contributes to senescence phenotype, evidenced by HDAC levels decreased upon senescence in human fibroblasts, and HDAC1/2 could lead to a delay in the onset of senescence [37,38].

Cellular senescence is the biological consequence of aging, implicated in a variety of age-associated diseases. These diseases share fundamental and unappreciated pathology at the cellular and genetic levels through cellular senescence [39]. Senescence may promote carcinogenesis in surrounding tissues by secreting a wide variety of factors, which alter the microenvironment to enhance growth of neighboring tumor cells [40]. On the other hand, emerging evidence suggests that cellular senescence also acts as a barrier to tumor progression, because senescence inhibits aberrant cell proliferation of cancer cells, decreases cell motility, and prevents the oncogenic transformation of primary human cells [41,42]. Therefore, senescence is thought to act as a double-edged sword for tumorigenesis [43].

3. Contribution of miRNAs and miRNA-regulated genes to senescence

The miRNAs are important regulatory molecules of gene expression regarding senescence. Specific overexpression or down-regulation of certain miRNAs has been shown to play a role in senescence through potentially targeting genes on the p53–p21 and p16–pRB pathways. For example, miR-34a overexpression during senescence can induce cell cycle arrest by targeting CDK4/6, Cyclin D1, E2F and SIRT1 [18,44,45]. miR-22, up-regulated in senescent cells, can negatively regulate the CDK6 and SIRT1 to induce cellular senescence [17]. In contrast, miR-24, which was down-regulated during senescence, was found to modulate cellular senescence by targeting p16 [46]. Other miRNAs (miR-16, miR-195, miR-107 and miR-185) that also directly repress CDK6 by binding to its 3′-UTR induce cell cycle arrest [47,48]. Recent reports

Please cite this article as: D. Xu, H. Tahara, The role of exosomes and microRNAs in senescence and aging, Adv. Drug Deliv. Rev. (2012), doi:10.1016/j.addr.2012.07.010

show that multiple miRNAs such as miR-17-5p, miR-20a/b, miR-93, miR-106a/b, miR-146a-b, miR-372 and miR-373 bypass Ras-induced senescence by directly targeting p21 [27]. Therefore, one miRNA can regulate several genes to cooperate in senescence, whereas many miRNAs can target one gene to control senescence (Fig. 1).

Traditionally, cellular senescence has been thought to arise as a consequence of altered gene expression including senescence genes, senescence suppressor genes, oncogenes, tumor suppressor genes, stemness genes, epigenetic genes and others (Table. 1). Cellular senescence can be triggered by telomere shortening due to the end replication problems in human somatic cells. Telomerase, a ribonucleoprotein enzyme for telomere elongation, is inactivated in normal somatic cells, but most cancer cells and stem cells have telomerase activity due to the activation of human telomerase reverse transcriptase (hTERT) gene. Although little is known about hTERT regulation by miRNAs, it is reported that miR-138 potentially targets the hTERT gene, involved in the development of thyroid carcinoma [49]. miR-128a was identified to directly target Bmi-1 oncogene, increasing p16 expression to promote cellular senescence [50]. The p53-independent up-regulation of miR-34a provoked senescence through repression of v-myc myelocytomatosis viral oncogene homolog myc [51]. miR-372 and miR-373 prevent Ras-induced senescence through the down-regulation of tumor suppressor LATS2 [52]. miR-21 modulates apoptosis by regulating Ras [53] and phosphatase and tensin homolog (PTEN)-dependent activation of PI 3-kinase signaling [54]. The miR-302-367 cluster acts after Oct4, Sox2 and Nanog to maintain stemness of human embryonic stem cells [55]. Let-7b is involved in decline of neuronal stem cell self-renewal during aging by reducing HMGA2 levels in old but not in young mice [56]. In addition, miR-146a can inhibit cellular senescence by targeting IL-6/8 [57]. The proto-oncogene LRF, leukemia/lymphoma related factor, is post-transcriptionally regulated by miR-20a, inducing senescence in mouse embryonic fibroblasts through preventing p19ARF transcription [16]. miR-29 and miR-30 can mediate repression of B-Myb expression during Rb activation, resulting in cellular senescence [58]. Some receptors such as ER [59] and ERBB2/3 [60] are regulated by miR-22 and miR-125, respectively. Above all, these miRNAs modulate cellular senescence through targeting various genes on p53/pRB pathway and/or other signaling pathways.

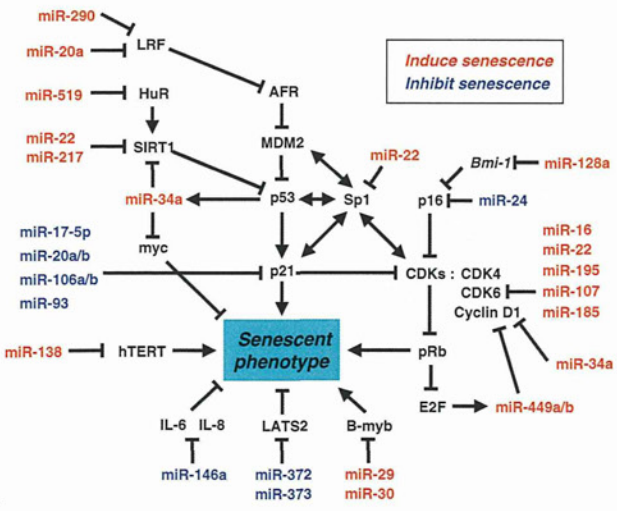

Fig. 1. miRNAs are involved in cellular senescence through p53/pRb pathway and other pathways. Cellular senescence is modulated by a variety of miRNAs as shown. These regulatory miRNAs induce senescence phenotypes (indicated in red) or delay the onset of senescence (indicated in blue).

Table 1
Genes associated with cellular senescence.

Genes	Functions	Examples	miRNAs	References
Senescence genes	Cell cycle regulators	p16	miR-24	[46]
		p21	miR-106a/b	[27]
Senescence suppressor genes	Regulators of telomere length	hTERT	miR-138	[49]
Oncogenes	Signal transduction molecules	Ras	miR-21	[53]
		Bmi-1	miR-128a	[50]
		myc	miR-34a	[51]
Tumor suppressor genes	Signal transduction molecules	p53	miR-34a	[44]
		LATS2	miR-372, 373	[52]
		PTEN	miR-21	[54]
Stemness genes	Self-renewal regulators	SOX2	miR302-367	[55]
		OCT3/4		
Epigenetic genes	Chromatin factors	HMGA2	Let-7b	[56]
	Histone modification	SIRT1	miR-22	[17]
Others	Inflammatory factors	IL-6, 8	miR146a	[57]
	Transcription factors	LRF	miR-20a	[16]
		Sp1	miR-22	[17]
		B-Myb	miR-29, 30	[58]
	Receptors	ER	miR-22	[59]
		ERBB2/3	miR-125a-5p	[60]

4. Involvement of secretory factors in cellular senescence

Senescent cells secrete not only exosomes but also other inflammatory cytokines and chemokines [61]. Recently, it has been reported that senescent cells assume a novel phenotype, the so-called senescence-associated secretory phenotype (SASP), which developed in normal fibroblasts, epithelial cells, and epithelial tumor cells after genotoxic stress in culture, and in epithelial tumor cells in vivo after treatment of prostate cancer patients with DNA damaging chemotherapy [62]. SASP is characterized by the secretion of myriad factors associated with inflammation and malignancy factors as well as the release of exosomes [21,43,62].

The secreted factors including matrix components, extracellular proteases, cytokines, and chemokines set the stage for crosstalk between senescent cells and their environment [63]. Of note, the effect of secreted factors is complex: they seem to reinforce the senescent phenotype in nearby senescent cells but at the same time can increase the proliferation of nearby neoplastic cells. For example, interleukin (IL)-6 contributes to the induction of senescence of nonmalignant cells in an autocrine manner [64], whereas its tumor promoting function by paracrine signaling has been proposed to directly or indirectly target the angiogenic compartment [65]. In cultured premalignant epithelial cells, SASPs induced an epithelial–mesenchyme transition and invasiveness, hallmarks of malignancy, by a paracrine mechanism that depended largely on the IL-6 and IL-8. Senescent cells contribute to induction of senescence in cells in its immediate vicinity mediated by secreted factors, which could constitute a danger signal that sensitizes normal neighboring cells to enter senescence, and block growth factors signaling directly by inhibition at the receptor level, thereby potentially contributing to the induction of senescence [66]. Tumor cells can misuse signaling of secreted factors, inducing senescence in fibroblasts. These senescent fibroblasts could in turn secrete factors that contribute to tumor growth in the later stage of tumorigenesis [67]. In addition, aging can lead to an increase in the number of senescent cells, thereby potentially stimulating expansion of premalignant cells [40]. Therefore, it is thought that cellular senescence suppresses tumorigenesis early in life, whereas it may promote cancer in aged organisms.

In addition to secretion of cytokines, senescent cells produce high levels of exosomes that are able to modulate the microenvironment during senescence. Exosomes are secreted by most cell types including dendritic cells, B cells, T cells, epithelial cells, and tumor cells, and interact with surrounding cells upon secreted. Exosomes can introduce

Please cite this article as: D. Xu, H. Tahara, The role of exosomes and microRNAs in senescence and aging, Adv. Drug Deliv. Rev. (2012), doi:10.1016/j.addr.2012.07.010

regulatory secreted factors into the interiors of the cells or receptors into the external membranes of the cells, providing intercellular communication both within and between cells [6]. Exosomes participate in the surface-membrane traffic and the horizontal transfer of protein and RNAs as well miRNAs among neighboring cells, which are necessary for the rapid phenotype adjustments in a variety of conditions. [68]. It is reported that senescence is associated with the release of exosomes, demonstrating a significantly increased release of exosome-like microvesicles during senescence in normal human fibroblasts. Importantly, senescence-associated exosomes were also observed to release from human senescent prostate cancer cells, suggesting senescence-associated exosomes can transfer cargos with both immunoregulatory potential and genetic information, between cells during cellular senescence [19]. EGFR is repressed at the chromatin level during senescence and is shown to be potentially regulated during cellular senescence [69]. Exosome-like microvesicles released by EGFR-bearing tumor cells are incorporated by neighboring endothelial cells, resulting in activation of the MAPK and Akt pathways and the autocrine production of VEGF. Their transfer between EGFR-bearing glioma cells can accelerate the growth of tumor cells that take up the vesicles. Thus, the effects of exosomal release in senescence could be wide ranging and influence the microenvironment [70].

The secretory activity and the release of exosomes in senescent cells are regulated by p53 tumor suppressor (Fig. 2) [71]. In cells undergoing senescence, p53 acts as a transcription factor and up-regulates a variety of secreted factors such as insulin-like growth factor-binding protein 3 (IGFBP-3). IGFBP3, secreted by some senescent cells, is known to be up-regulated in senescent fibroblasts and endothelial cells, leading to senescence [71,72]. In addition, it is reported that p53 up-regulates tumor suppressor-activated pathway-6 transcript (TSAP6), which is an intracellular factor that stimulates exosome release into the extracellular medium [71,73]. Chmp4 that recruits Alix protein to the endosome to function in MVB vesicle formation is also induced by p53 activation [74]. The p53 protein can also activate caveolin-1, the main component of the caveolae plasma membranes, and facilitate the endocytosis, accompanied with endosomal clearance of membrane receptors from cell surface [74,75] . In addition, overexpression of caveolin-1 induced premature senescence in human fibroblasts [76], whereas knockout of caveolin-1 by shRNA blocks the induction of bleomycin-induced senescence [77]. Maspin, a mammary serine protease inhibitor, is also up-regulated by p53 in response to stress, and plays a role in the exosome secretion [71]. At present, it is well known that both secreted factors and exosomes are secreted from senescent cells, and involved in a variety of biological function, but it is still unclear whether they coordinately influence each other for the biological effects of age-associated diseases.

5. Biological processes mediated by miRNAs and exosomes during senescence

Recent findings have revealed the complexities of the senescence phenotypes, demonstrating that senescent cells differ from proliferating cells in three way: (1) they arrest cell growth and cannot be stimulated to reenter the cell cycle by known physiological stimuli; (2) they become resistant to apoptotic cell death; (3) they acquire altered differentiated functions [21,78]. All of these changes might result from cooperative changes in multiple systems with the resultant changes to pathways regulating different cellular processes.

The ability of miRNAs to regulate a variety of target genes allows them to induce changes in multiple biological processes, implicating that miRNAs may provide a significant link between senescence and other biological processes. Using the systems biology tool Metacore from Genego, pathway analysis of senescence-associated miRNA targets demonstrates the common signaling pathways resulting in senescence [79]. Dhahbi et al. used DAVID and Gene Ontology to functionally annotate miRNA-regulated genes, revealing the biological processes targeted by miRNA expression changes during senescence [80]. Among them, the most highly represented and enriched term is regulation of cell proliferation, which is consistence with a pivotal role of miRNAs in cell proliferation regulation since inhibition of proliferation is the hallmark of senescence [21]. Senescence-associated miRNAs, miR-22 and miR-34a

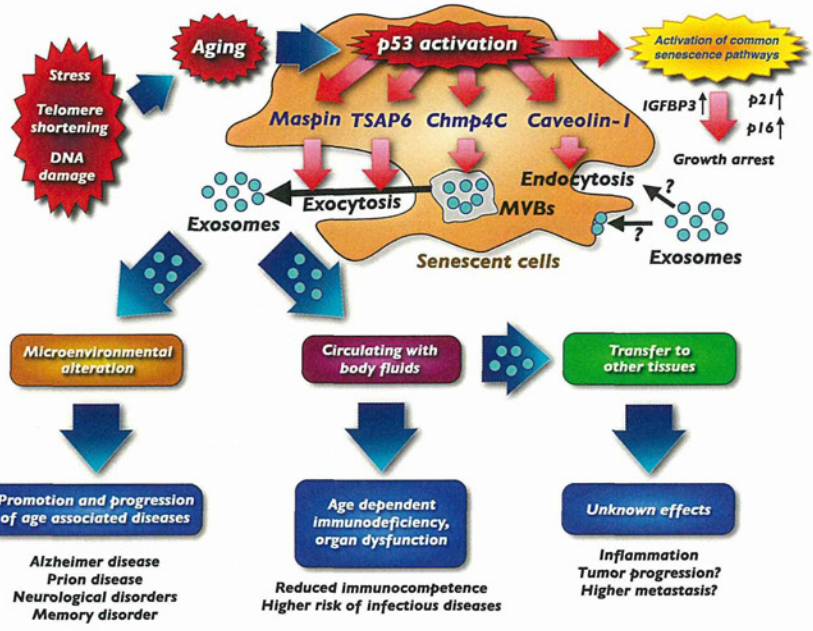

Fig. 2. The secretory activity and the release of exosomes are regulated by p53 tumor suppressor in senescent cells. Senescence-inducing factors such as oxidative stress, telomere shortening and DNA damage induce p53 activation followed by the increase in p21, p16 or IGFBP3 on the senescence pathways. The activation of p53 also induces up-regulation of Maspin, TSAP6, Chmp4C and Caveolin-1, which can enhance the endosome production, the exosome production and release from the plasma membrane. Higher production of exosomes which cargo miRNA and proteins from senescent cells may induce the alteration of microenvironment in age-associated diseases, cause immunodeficiency and organ dysfunctions in infectious diseases, and result in other unknown effects such as inflammation.

Please cite this article as: D. Xu, H. Tahara, The role of exosomes and microRNAs in senescence and aging, Adv. Drug Deliv. Rev. (2012), doi:10.1016/j.addr.2012.07.010